Synthesis of *Pf*CLK1 Inhibitors

Shaun Eganda (xxxxxxxx) - 2022-2023

Academic Supervisor – Prof. Andrew Jamieson

Industry supervisor – Dr Maxime Rouah

2.0 Acknowledgement

I want to thank my primary supervisor, Professor Andrew Jamieson, for his guidance throughout the project. I would also like to thank my industry supervisor, Dr. Maxime Rouah, for being available to answer my questions, encouraging me when my chemistry in the lab was not working, and advising me on how to best manage my time. Most importantly, I would like to thank the Holy Spirit for encouraging me throughout and bringing me to the end of the project.

3.0 Abstract

Despite international efforts to deal with malaria, it remains a serious health concern on a global scale, contributing to a considerable number of deaths worldwide, especially in LEDCs (less economically developed countries) on the African and Asian continents. Unfortunately, a lack of research has resulted in no new antimalarial drugs being introduced into the market since 1996. Current treatment strategies against malaria have been seen in the form of artemisinin; however, due to constant usage, this drug has become compromised, as the most virulent malaria parasite strain, *Plasmodium falciparum,* has developed resistance. As a result, significant efforts must be targeted towards the development of new antimalarial drugs that target not only the symptomatic blood stage of infection, but all stages of the parasite life cycle to prevent transmission and hopefully allow the eradication of malaria.

In recent times, a four-membered protein kinase family known as '*Plasmodium falciparum* cyclin-like kinase' (*Pf*CLK1-4) has been identified as an essential eukaryotic protein for the survival of the parasite during the 'blood stage' of its lifecycle. Studies have shown these kinases to be pivotal in regulating RNA expression throughout the asexual and sexual stages of the parasite lifecycle, which are important in parasite survival. As a result, efforts have been made to focus on this protein kinase family to see if targeting these protein kinases could offer a novel therapeutic strategy to treat malaria. Henceforth, this project aims to validate one of these family members '*Pf*CLK1 as a new therapeutic target against malaria by synthesizing tool compounds that selectively inhibit *Pf*CLK1.

As this project is still in the early 'hit to lead' stage of the drug discovery process, the focus so far has been on developing a synthetic route towards the 'hit' molecules identified from a HTS (high throughput screen) that showed biological activity against *Pf*CLK1. As a result, the main discussion of this report will outline the synthetic route used to synthesize two of the four hit molecules, compounds A & B. **Figure 1**

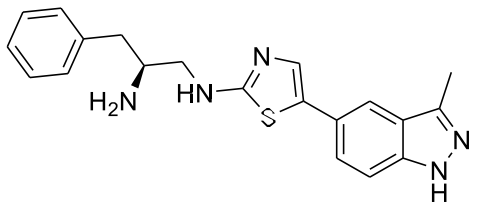

A

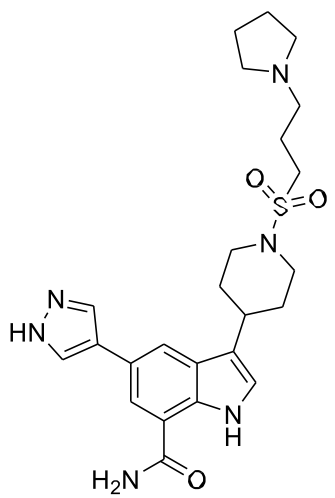

B

Figure 1 – Structures of HIT compounds A & B

4.0 - Abbreviations

ACTs: Artemisinin combination therapies

Et_2O: Diethyl ether

COSY: Correlated spectroscopy

DCM: Dichloromethane

DEPT: Distortionless enhancement by polarization transfer

EtOAc: Ethyl acetate

HRMS: High-resolution mass spectroscopy

Hrs: Hours

HTS: High-throughput screening

IR: Infrared spectroscopy

LC-MS: Liquid chromatography mass spectrometry

LEDC: Less economically developed countries

MP: Melting point

NTD: Neglected tropical disease

PET Ether: Petroleum ether 40-60 °C

P*f*CLK1: Plasmodium falciparum cyclin-dependent kinase-like Kinase

WHO: World Health Organization

THF: Tetrahydrofuran

Table of Contents

5.0 Introduction

5.1 - Neglected Tropical Diseases and Diseases of Poverty

Neglected tropical diseases (NTDs) are a class of diseases commonly found in tropical areas and affect predominantly low-income communities within less developed countries. These diseases are commonly caused by bacteria, viruses, parasitic worms, protozoa, and snake venom.[1] Malaria, although a tropical disease, differs slightly from other NTDs due to the large investment that has been made and continues to be made towards treatment procurement, research, and development. Despite these efforts, the challenges to ending malaria are the same as other NTDs. Firstly, small commercial markets due to drug beneficiaries coming from low-income communities make investing in drug discovery and translational activities unappealing to the pharmaceutical industry, as they would ultimately be loss-making markets unless robust risk and cost-sharing strategies are developed.[2] As a result, a lack of affordable and effective medication against these diseases has been identified. However, there have been notable efforts by pharmaceutical companies to donate drugs to help overcome this challenge. Examples include those by Merk KGaA, GSK, Eisai, and Merck & Co., whose efforts in supplying anti-parasitic drugs like ivermectin, praziquantel, albendazole, and diethylcarbamazine have aided the governments of these affected nations in tackling the problem.[2] Secondly, there is always the intrinsic risk of pathogenic drug resistance when treating infectious diseases; this provides additional scientific challenges, as continued drug development will be needed to treat new pathogen variants in the future. Thirdly, there are additional chemistry challenges that come from having to deliver low-cost medicines that are simple to administer and often require pediatric formulation, problems not typically considered in the first-world drug discovery process. Product Development Partnerships (PDPs) such as the Drugs for Neglected Diseases Initiative (DNDi) and the Medicines for Malaria Venture (MMV) were established over 20 years ago to address failure in the market by large pharma[2]. PDPs like MMV which are donor-funded organizations that focus solely on developing and delivering medicines against malaria, have made great strides in the effort to eradicate malaria, the disease that this report will be discussing.

6.0 Malaria

6.1 - Disease Overview

Malaria is an infectious parasitic disease caused by the unicellular eukaryotic apicomplexan parasite *Plasmodium*.[3] *Plasmodia* species can infect numerous vertebrate and insect species; however, six species are known to infect humans: *P*. falciparum, *P*. vivax, *P*. ovale (sub-species, *P*. ovale curtisi and *P*. ovale wallikeri), *P*. malariae, *P*. knowlesi, and *P*. cymomolgi, though infection with the latter is extremely rare.[3] Of these, *P*. *falciparum* is the most lethal and is responsible for the majority of mortalities in Africa. *P*. vivax, on the other hand, is responsible for over 65% of malaria cases in South America and Asia.[3] In 2020, an estimated 229 million global cases of malaria and 409,000 deaths were reported, of which 67%[3] were children under the age of 5 years. Furthermore, other sources have suggested that the number of asymptomatic but infected people is far greater than what is statistically reported in the literature. The severity of malaria can further be characterized by a concept known as disability-adjusted life years (DALYs). DALYs is a system that measures the premature mortality, prevalence, and severity of malaria in a country.[2] In 2017, the age-adjusted DALYs for malaria were estimated at 45 million, but it is important to note that this is a 34% improvement compared to 2007 figures.[2]

Organizations such as the United Nations have developed and are enforcing sustainable development goals to end global malaria epidemics. The World Health Organization global technical strategy for malaria has set the goal to reduce cases and mortality by 90% by the end of 2030, as well as ambitiously eradicate the key malaria parasites.[2] These goals could be realized, with more countries globally moving towards zero indigenous cases as a strong indicator, as well as a decrease in the number of countries with fewer than 100 indigenous cases (17 countries in 2010 vs. 27 countries in 2019), which shows that elimination is within reach as predicted. Despite these promising results, five countries account for over 50% of all worldwide malaria cases (Nigeria 27%), the Democratic Republic of the Congo 12%, Uganda 5%, Mozambique 4%, and Niger, 3%), showing that there is still a way to go until the vision of complete eradication is realized.[4]

6.2 - *Plasmodium* Lifecycle

Malaria occurs when a female Anopheles mosquito that has been infected with the *Plasmodium* parasite transmits this parasite to a human during blood feeding **Figure 2**. During feeding, the infected mosquito injects approximately 100 *Plasmodium* sporozoites (the earliest form of the *Plasmodium* parasite) into the skin, which then burrow into blood vessels and travel to the liver, where they infect hepatocyte cells (15–30min).[2] Asymptomatic asexual replication is initiated, which results in clonal expansion, whereby, in under 6 days (in the case of *falciparum*), a single sporozoite that made a successful invasion of the hepatocyte cell is able to asexually replicate itself into 40,000 new parasites (merozoites). Eventually, a build-up of parasites within the cell causes the hepatocyte cells to lyse, releasing merozoite parasites into the blood stream.

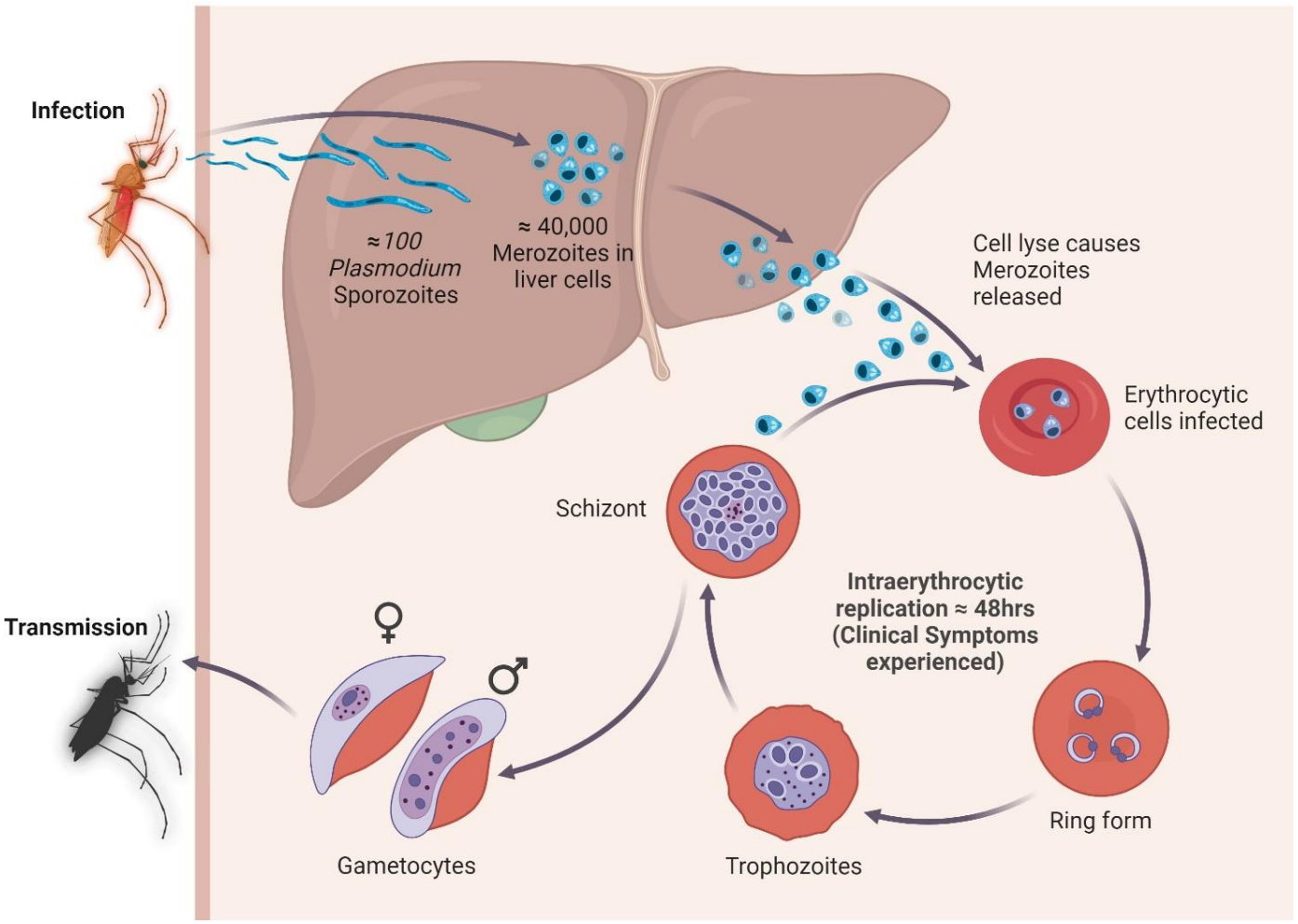

Figure 2 – Malaria transmission mechanism

In the case of hepatocyte cells infected with *P*. vivax, differentiation into hypnozoites causes the parasites to remain dormant and not partake in the first round of infection. After time, *P*. vivax hypnozoites (the dormant *P*. vivax parasite) can relapse to form liver schizont (daughter hypnozoites) and progress to a blood-stage infection.[2] This mechanism allows *P*. vivax to wait out long and dry winter seasons when mosquitoes are not present to spread disease. While *P*. falciparum forms dormant hypnozoites, they can also cause asymptomatic infections that allow them to be dormant during the dry season in Sahel countries.[5]

Once in the bloodstream, merozoites infect erythrocyte cells and initiate intraerythrocytic replication. While asexual replication in the human liver stage is asymptomatic, after 48 hours of infecting erythrocyte cells, victims begin to experience clinical symptoms such as fever.[2] A single merozoite can produce 20–32 new merozoites within the erythrocyte cell, resulting in cell lysis. A small percentage of these new merozoites progress into gametocytes, the male and female sexual stages of the parasite, which are eventually taken up by another mosquito, causing the cycle to repeat itself during blood feeding.[2]

Within the female anopheles, mosquito gametocytes reproduce sexually to form a diploid zygote that differentiates into ookinete, then oocyst, these liberate into new sporozoites that migrate to the mosquito's salivary glands, ready to infect at the next blood feeding.[6] The whole mosquito parasite stage takes up to 14 days. Initial symptoms of malaria in humans are non-specific, resembling those of a typical flu infection. Sufferers may experience headaches, nausea, muscle pains, diarrhea, fever, and chills. The defining symptom, however, commonly described by most sufferers is a fever followed by shivering and chills, which is synchronous with merozoites leaving their host cells and infecting erythrocyte cells[7,8] If treated with appropriate medication, these symptoms should subside over a few days, but if left untreated can prove fatal.[9]

7.0 Severe Malaria

7.1 - Cerebral malaria

Cerebral malaria is the most severe neurological complication associated with the *falciparum* parasite.[10] Cerebral malaria results in impaired consciousness and, in more extreme cases, coma. The cause of cerebral malaria is when parasite erythrocytes are sequestered in the cerebral microvasculature.[10] This results in the swelling of the brain, retinal changes, and abnormalities in posture and breathing.[11] Cerebral malaria, without immediate medical intervention, is habitually fatal. However, even with treatment, 15–25% of infected children die.[12] Additional studies show that children who survive have an increased risk of neurological and cognitive defects, behavioral challenges, and epilepsy.

7.2 - Anemia

In malaria-endemic areas, severe anemia is the main symptom of severe malaria. Increased hemolysis of red blood cells following infection by merozoites decreases hemoglobin levels, resulting in anemia.

7.3 - Malaria in Pregnancy

Pregnant women are significantly more likely to develop severe malaria in comparison to their non-pregnant counterparts, with those suffering from severe malaria having a mortality rate close to 50%.[10] In endemic areas, it has been estimated that at least 25% of those with malaria are pregnant women, with first-time mothers being most at risk, along with adolescents and HIV-infected patients. Reasons for the higher occurrence of malaria among pregnant women can be attributed to increased parasite sequestration, as the placenta offers another site of parasite attack.[10,11] Additional sequestration results in pregnant women suffering disproportionately from anemia, resulting in high risks of mortalities such as congestive heart failure and hemorrhage during childbirth.[10] Malaria of the placenta can also result in complications for the fetus, resulting in stillbirth, babies of low weight at birth, and intrauterine growth restrictions.[10]

8.0 Treatment of Malaria

8.1 - Artemisinin Combination Therapies

Traditional treatments for severe malaria consist of using a combination of chloroquine **1** and sulfadoxine-pyrimethamine **2, Figure 3**. Malaria-endemic regions, however, opt to use mefloquine **3,** lumefantrine **4**, and amodiaquine **5** as their antimalarial drug of choice for no other reason than their availability and affordability. However, with the additional side effects associated with mefloquine, chloroquine, and lumefantrine, combinations are traditionally a safer option.[13]

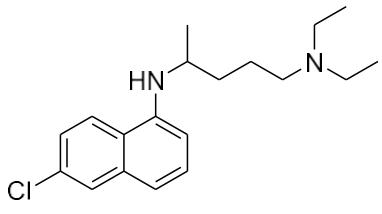

1

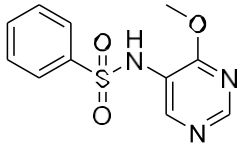

2

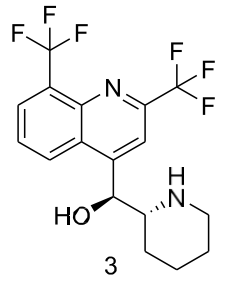

3

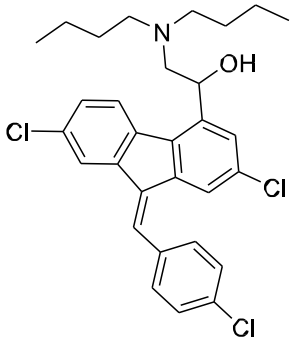

4

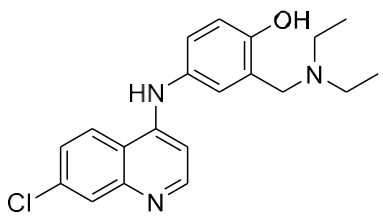

5

Figure 3 - Chloroquine **1** and a selection of antimalaria partner drugs found in Artemisinin combination therapies (ACTs): sulfadoxine-pyrimethamine **2**, mefloquine **3**, lumefantrine **4**,

amodiaquine **5**.

As time has progressed, resistance to these traditional antimalarial drugs has made these treatments redundant, and thus the development of new antimalarials in the form of artemisinin derivatives came into existence.[14]

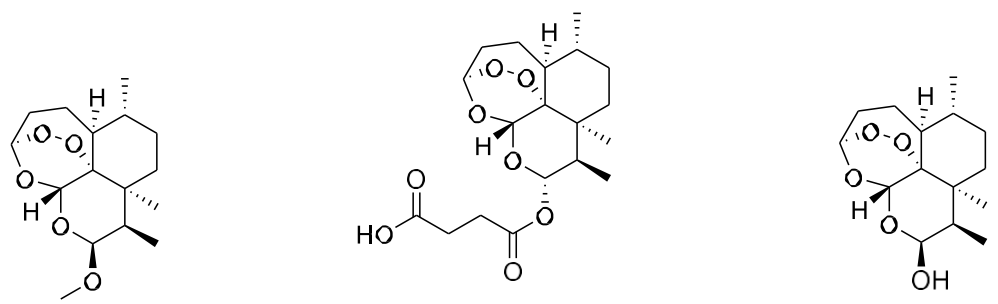

6 **7** **8**

Figure 4 - Artemisinin Derivatives

The 1990s saw the introduction of artemisinin derivative compounds **6, 7, 8** as the next revolutionary antimalaria drug. With severe malaria being unresponsive to traditional antimalarial medication as a result of parasitic resistance, artesunate **6**, **Figure 4** was the main drug of choice against severe malaria, administered intravenous or intramuscularly.[14] However, orally administered artemisinin-based combination therapy (ACTs) was advised by the World Health Organization as the best form of treatment against uncomplicated *Plasmodium falciparum* malaria; due to safety and its effectiveness against other species of the *Plasmodium genus***.**[14] These artemisinin derivatives are used in combination with slower-acting prodrugs, **Figure 3.** ACTs as a whole have been seen as being effective against 90% of malaria.[12] The rationale behind having an artemisinin and a secondary drug is that fast-acting artemisinin will rapidly kill the majority of the parasites over a short period (via a mechanism distinct from the partner drug), and thereafter, the partner drug will kill any remaining parasites over a longer period due to its slow-acting nature. This allows for even parasites that have become resistant to artemisinin to be killed.[15]

Artemisinin is a sesquiterpene lactone containing an endo-peroxide bridge.[16] Though the actual mechanism showing how artemisinin kills malaria parasites is not known, the opening of this endo-peroxide bridge via a hemoglobin group is essential for killing the malaria parasite **Scheme 1.** During the blood stage, host hemoglobin is the primary food source for the malaria parasite. Once digested, the malaria parasite releases the hemoglobin group as a by-product of hemoglobin digestion, and this acts as a source of iron for activating artemisinin.

Artemisinin and its derivatives are prodrugs that when subjected to a heme group, undergo endoperoxide cleavage. According to the reductive scission model, the binding of a ferrous atom to the drug and a single electron transfer facilitates the cleavage of the peroxide bond in compound **9**, resulting in an oxygen-centered radical compound **10**. This O-centered radical can undergo a 1,5 – H shift to generate a C-centered free radical.[16,17] Once formed, the free radical **11** can interact with biomolecules, resulting in membrane damage, alkylation, and inhibition of protein and nucleic acid synthesis, all of which result in parasite death.[17]

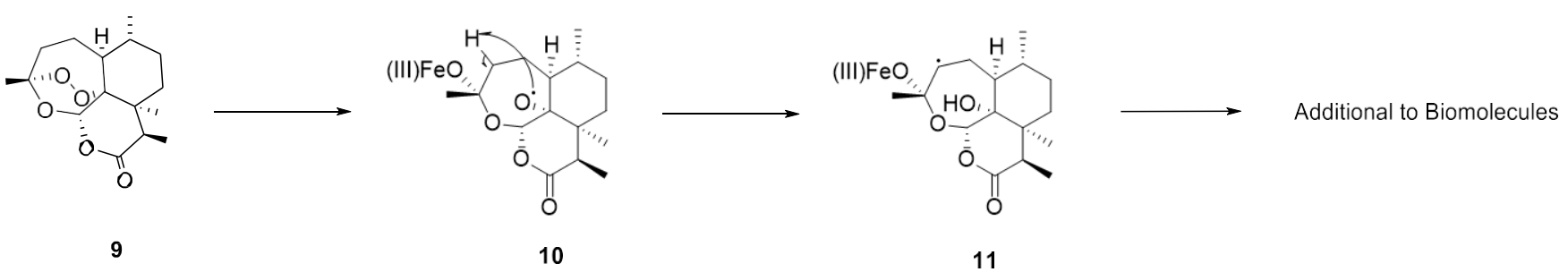

Scheme 1: Proposed bioactivation of artemisinin: reductive scission model.[17]

9.0 Protein kinases

9.1 - Protein Kinases Structure & Function

Protein kinases (PKs) are an essential class of enzymes that regulate the selective phosphorylation of protein substrates, resulting in a change in the function of the substrate.[18] This special group of enzymes are important because they are responsible for the regulation of most signaling events in the eukaryotic cell life cycle.[18] Protein kinases in eukaryotic cells can be classified into five major groups based on the amino acid residues they phosphorylate. Some of these are serin/threonine protein kinases (ST-PKs), tyrosine protein kinases (TKs), histidine-specific kinases, dual-specificity protein kinases, and aspartic/glutamic acid-specific protein kinases. Two to four of these five are serine/threonine protein kinases and tyrosine kinases. They phosphorylate hydroxyl groups on serine and threonine amino acid residues and phenolic hydroxyl groups on tyrosine substrates. The catalytic functionality of protein kinases is contained within structurally conserved catalytic domains called kinase domains**.**[19] Within this kinase domain, twelve catalytic subdomains span two distinct lobes: an *N*-terminal lobe that anchors the nucleotide, and a larger *C*-terminal lobe that binds the substrate and initiates phosphorylation.[19] A cleft in the *N*-terminal lobe and *C*-terminal lobe forms the catalytic site of the kinase. Kinase domains make sure that adenosine triphosphate (ATP) and the peptide substrate are in the right place before ATP's γ-phosphate group is transferred to an acceptor amino acid in the protein substrate.[20,21]

9.2 - *Plasmodium falciparum* Kinome

Given that protein kinases play a major role in eukaryotic cellular processes, a great interest emerged in sequencing the *Plasmodium falciparum* genome to determine whether protein kinases play a significantly important role in the *P. falciparum* lifecycle.[22] Results from the *P. falciparum* genome sequence revealed that 66% of the genes could not be assigned to any specific function; this was validated by directly comparing the sequence homology with characterized genes from other genomes.[23,24]

10.0 *Pf*CLK3

A 2011 study combined phospho-proteomic analysis with kinome-wide reverse genetics to determine the importance of protein phosphorylation in *Plasmodium falciparum* asexual proliferation.[25] The study identified 1177 phosphorylation sites on 650 proteins essential to a wide range of general cellular activities, including DNA synthesis, transcription, and metabolism, as well as key parasites.[25] Following this discovery, it was decided to target the protein *Pf*CLK3, as it was shown to regulate RNA processes essential for malaria parasite survival in the asexual blood stage of the life cycle. *Pf*CLK3 is a member of the *Plasmodium falciparum* protein kinases family (*Pf*CLK1-4) and is a tyrosine kinase that self-phosphorylates and then becomes a serine/threonine kinase that can phosphorylate sarcoplasmic reticulum proteins which are involved in RNA splicing.[25] As *Pf*CLK3 is important in mRNA processing, it strongly indicates that by inhibiting this kinase, the parasite will die at any stage of the life cycle where RNA processing is required; whether that be the liver, blood, or mosquito stages **Figure 2.**

Following the potential of *Pf*CLK3 as a new therapeutic target against malaria, Alam et al. in 2019 developed a high-throughput time-resolved fluorescence resonance energy transfer (TR-FRET) assay of *Pf*CLK3 and another similar isoform *Pf*CLK1.[26] The high-throughput assay was used to screen 24,619 compounds from the MRCT-index library, the GSK Tres Cantos Anti-malarial set (TCAMs), the GSK protein kinase inhibitor set (PKIS), and the medicines for Malaria Venture (MMV) malaria box.[26] Results showed 29% of hits specifically inhibited *Pf*CLK1, 13% inhibited *Pf*CLK3, and 58% inhibited neither kinase.[26] One compound, TCMDC-135051 **12, Figure 5**, showed high selectivity and potency against *Pf*CLK3, which prevented the maturation of trophozoite-to-schizont during blood-stage replication **Figure 2**, thereby stopping the next cycle of invasion.[26] *Pf*CLK3 inhibition was also shown to disrupt the transcription of genes responsible for kinases involved in splicing.[26] Transcriptional studies of TCMDC-135051 showed very few off-target events, which was interesting considering its proposed binding mechanism was type I.[26] Type I inhibitors tend to bind less specifically due to the conserved nature of the ATP binding site.

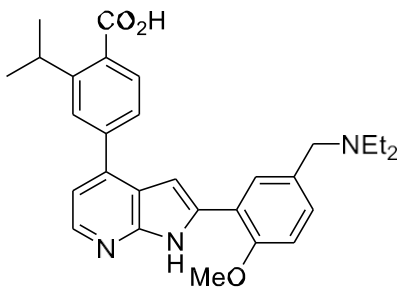

12

Figure 5: Structure of TCMDC-135051.

11.0 *Pf*CLK1

*Pf*CLK1 displays the same *plasmodial* homology as the mammalian Lammer Kinase. Additionally, like *Pf*CLK3, *Pf*CLK1 was identified as being essential for the parasite's survival and transmission. Additionally, *Pf*CLK1 has a similar function in that it is involved in the phosphorylation of SR-rich splicing factors, which are paramount for the correct assembly and catalytic activity of spliceosomes.[25] Spliceosomes themselves delete introns from pre- mRNA to form mature mRNA, an important process for transcription and, hence, cell proliferation.[25] Alam et al. showed that during the parasite blood stage, *Pf*CLK1 is primarily localized in nuclear speckles, where pre-mRNA splicing factors are localized and sent to sites where transcription is required.[25] The prevalence of *Pf*CLK1 in passages between the cytoplasm and the cell nucleus further supports its involvement in mRNA splicing and shuttling. This study went on further to confirm its importance in erythrocytic asexual replication, which, just like *Pf*CLK3, gives good grounds for it as an important chemotherapeutic target against malaria.

As previously discussed, Alam et al. in 2019 developed a (TR-FRET) assay where 24,619 compounds were both screened against *Pf*CLK3 & *Pf*CLK1.[25] To progress to phase 2 of the screen, compounds needed to meet a potency of 40% inhibition; this left 2838 compounds. The final phase of screening identified 4 hit compounds with nM potency for P*f*CLK1, as seen below in **Figure 6.**

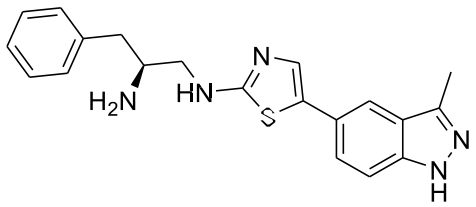

A

IC_{50} (*Pf*CLK1) = 7.1 nM

IC_{50} (*Pf*CLK3) = 400 nM

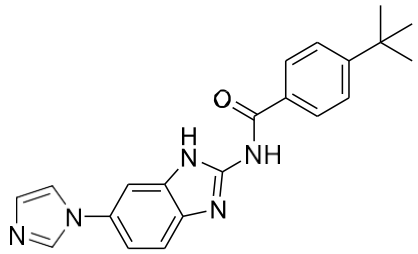

13

IC_{50} (*Pf*CLK1) = 25 nM

IC_{50} (*Pf*CLK3) = 2000 nM

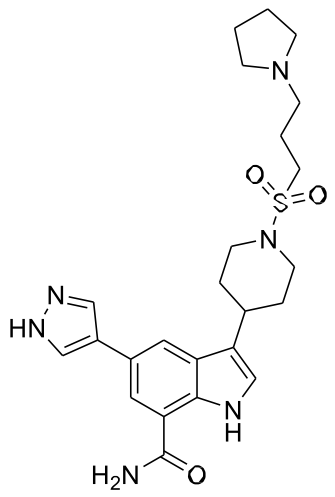

B

IC_{50} (*Pf*CLK1) = 190 nM

IC_{50} (*Pf*CLK3) = 2100 nM

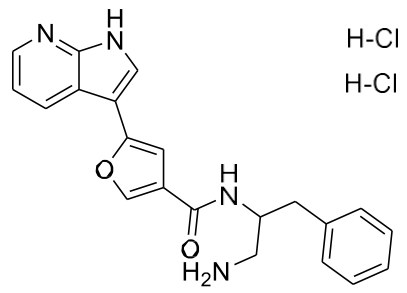

14

IC_{50} (*Pf*CLK1) = 40nM

IC_{50}(*Pf*CLK3) = 2300 nM

Figure 6: Structure of PfCKL1 selective Inhibitors identified from HTS of the following libraries: MRCT-index library, the GSK Tres Cantos Anti-malarial set (TCAMs), GSK protein kinase inhibitor set (PKIS), and the medicines for Malaria Venture (MMV) malaria box

12.0 Medicinal Chemistry

The pharmaceutical industry has significantly changed its sources of medication leads, utilizing natural products, patents, clinical observations, and academic collaboration.[27] High-throughput screening (HTS) has enabled the screening of numerous chemicals, overcoming the technical limitations of previous methods. (HTS) compounds that were previously difficult to dissolve into solution can now be dissolved in DMSO, enabling the evaluation of insoluble medicines.[27] The 'hit to lead' step in drug discovery synthesis involves constructing numerous compounds based on an ideal molecule that already has high potency, with minor changes tested in vitro to explore target receptor locations. From this, chemists can identify the best candidate compounds with in vitro efficacy and favorable absorption, distribution, metabolism, excretion, and toxicity profiles. High potency and selectivity are crucial for success, with IC_{50} numbers representing the amount of the drug required to elicit 50% inhibition of the target in vitro, and EC_{50} values indicate the 50% maximum action concentration of a substance.

Lipinski established the 'Rule of 5' in 1997 after studying several marketed oral medicines.[28] The 'Rule of 5' outlines guidelines that should be followed to increase the likelihood that a candidate molecule will show good oral exposure:

- **5 or fewer** hydrogen bond donors (e.g., OH, NH)
- **10 or fewer** hydrogen bond acceptors (e.g., O and N)
- **A logP** value between +5 and -5
- A **molecular weight** that is less than 5

Due to the lipophilic nature of a cell, phospholipid bilayer drug lipophilicity is one of the most crucial factors to consider when designing a drug whose target is within the cell. With this in mind, it is important to limit the number of hydrogen bond donors and acceptors in a molecule to ensure easy entrance into the cell.[28] In addition to this, research shows that increasing molecular weight reduces intestine and blood-brain barrier permeability, hence Lipinski rules advise a molecular weight limit of 500 or less.[28] Furthermore, because cell membranes are amphiphilic, prospective compounds must have a balance of hydrophilic and hydrophobic characteristics to successfully cross this layer. To examine this equilibrium, the octanol-water partition constant (P) is used, with the value commonly stated as the logP value Equation 1.

$$Logp = Log_{10}\frac{[Drug\ in\ Octanol]}{[Drug\ in\ Water]}$$

Equation 1: Calculation of logP[28]

However, for charged molecules, logD Equation 2 is a more accurate measure of lipophilicity since it considers the distribution of a chemical between a hydrophobic and aqueous solution at a specific pH (e.g., pH 7.4 under physiological conditions). As a result, this value will vary depending on the molecule's capacity to ionize.

$$LogD = logP + \log\left[\frac{1}{(1 + 10^{pka-pH})}\right]$$

Equation 2: Calculation of logD for a neutral base where pKa is the pKa of its conjugate acid.

The molecule's lipophilicity must be optimized, as a drug molecule that is too lipophilic cannot be absorbed into the bloodstream by the body, resulting in increased metabolism by the liver. At the same time, if the molecule is not lipophilic enough, it will not easily permeate across the cell membrane. A logP value between -5 and 5 ensures successful passage across the cell membrane, as well as solubility within the cell. Despite the Lipinski ‘Rule of 5’ providing a valuable set of standards to work towards for medicinal chemists, these should be viewed as guidelines rather than requirements for every possible therapeutic molecule.

The ligand efficiency (LE) of a molecule is another significant parameter in medicinal chemistry. This is a measure of the binding energy of a chemical to its receptor per non-hydrogen atom.[29] LE values are used to compare molecules to find the best lead compounds with the best combination of pharmacological and physicochemical features Equation 3.

$$\boldsymbol{LE} = \frac{1.37\ x\ \mathrm{pXC50}}{\mathrm{Heavy\ atom\ count}}$$

Equation 3: Calculation of ligand efficiency, X_{50} refers to either EC_{50} or IC_{50}.[30]

Lipinski's rule of 5 serves as a good criterion for medicinal chemists in the initial stages of drug discovery in predicting drugs that will be successful. However, over recent years, there has been an increase in drugs that do not comply with the Lipinski rule of 5 that have made it to market, such as venetoclax, which are BH3 mimetics that selectively target Bcl-2 and are utilized for their pro-apoptotic properties against chronic lymphocytic cancer.

13.0 Results & Discussion

13.1 Project Aims

Following the successful work to validate P*f*CLK3, this project aims to synthesize tool compounds to investigate whether P*f*CLK1 is also a suitable target to treat malaria. Like *Pf*CKL3, *Pf*CLK1 regulates RNA processing, an important process that occur across multiple stages of the parasite life cycle; therefore, there is a good chance that *Pf*CLK1 will be a good biological target against malaria. In addition, knowledge acquired from the *Pf*CKL3 study, the availability of tool compounds from high-throughput screening Figure 6, and published crystal structure images of the *Pf*CKL1 kinase domain provide an excellent starting point for the project. This project aims to apply innovative molecular design and advanced chemical synthesis methodology to develop a novel class of inhibitors selectively targeting *Pf*CLK1. Specific objectives include:

1. Synthesize the four hit molecules from the HTS Figure 6.

2. Establish inhibitory potency (TR-FRET) and in vivo antiparasitic activity (3D7 *Falciparum* parasites).

3. Perform molecular docking to investigate the mechanism of binding.

4. Recombinantly express *Pf*CLK1.

5. Screen covalent fragment libraries and hit compound scaffolds to develop potent and selective covalent inhibitors.

The retrosynthetic disconnections described below were used, primarily, to enable a rigorously regioselective forward synthesis based on well-established chemical transformations in the literature.

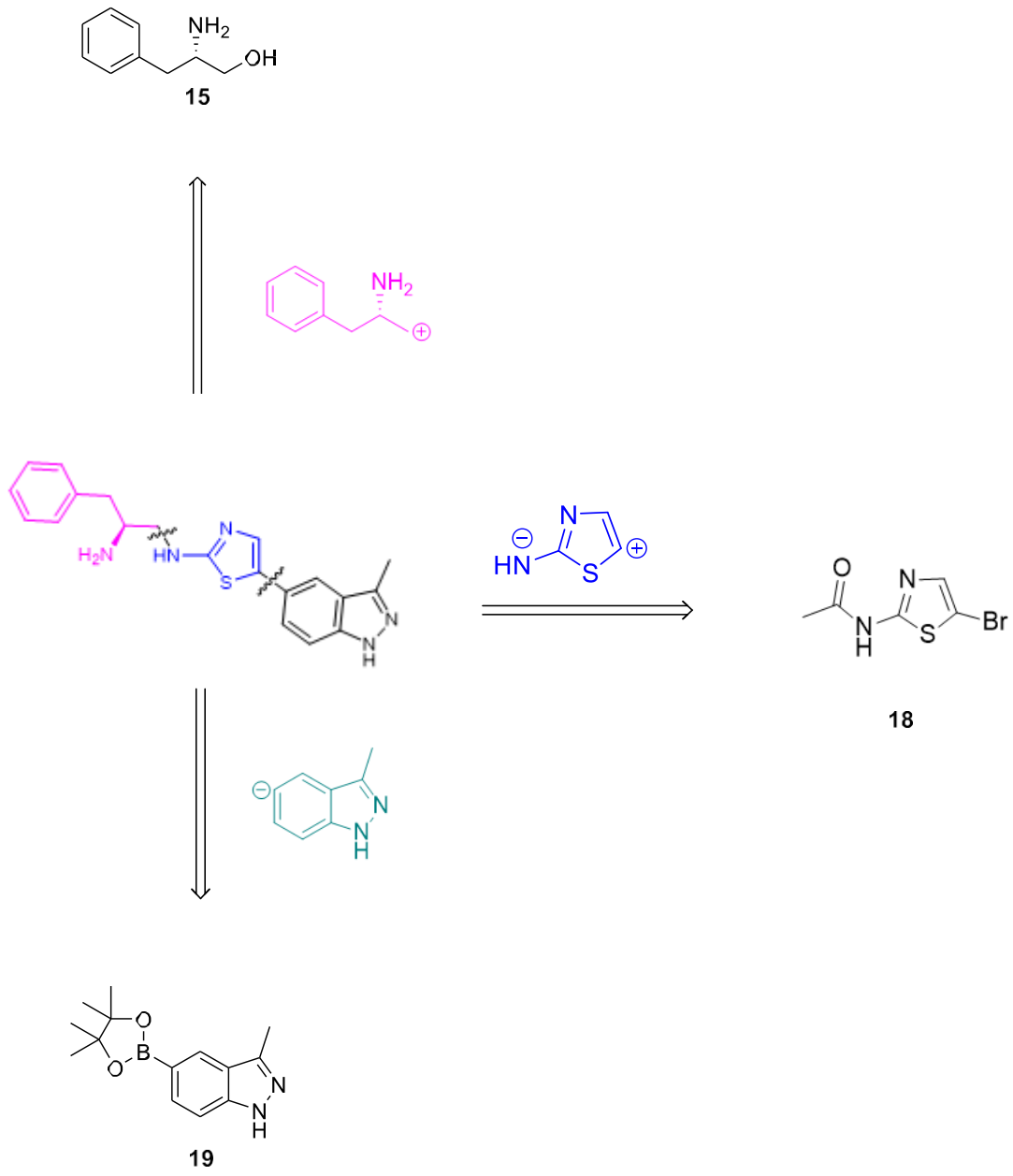

Scheme 2: Retrosynthesis of compound A

Regarding physicochemical properties, compound A complies with Lipinski's rules as it has a molecular weight of < 500 g mol^{-1} (363 g mol^{-1}) and the appropriate number of hydrogen bond donors and acceptors. High-throughput screening identified JZ208105-178D1 as having a pIC_{50} value of 7.1, showing high potency against *Pf*CLK1 as an initial hit compound and good ligand efficiency of 0.37 based on **equation 3.**

14.0 - Synthesis of compound A

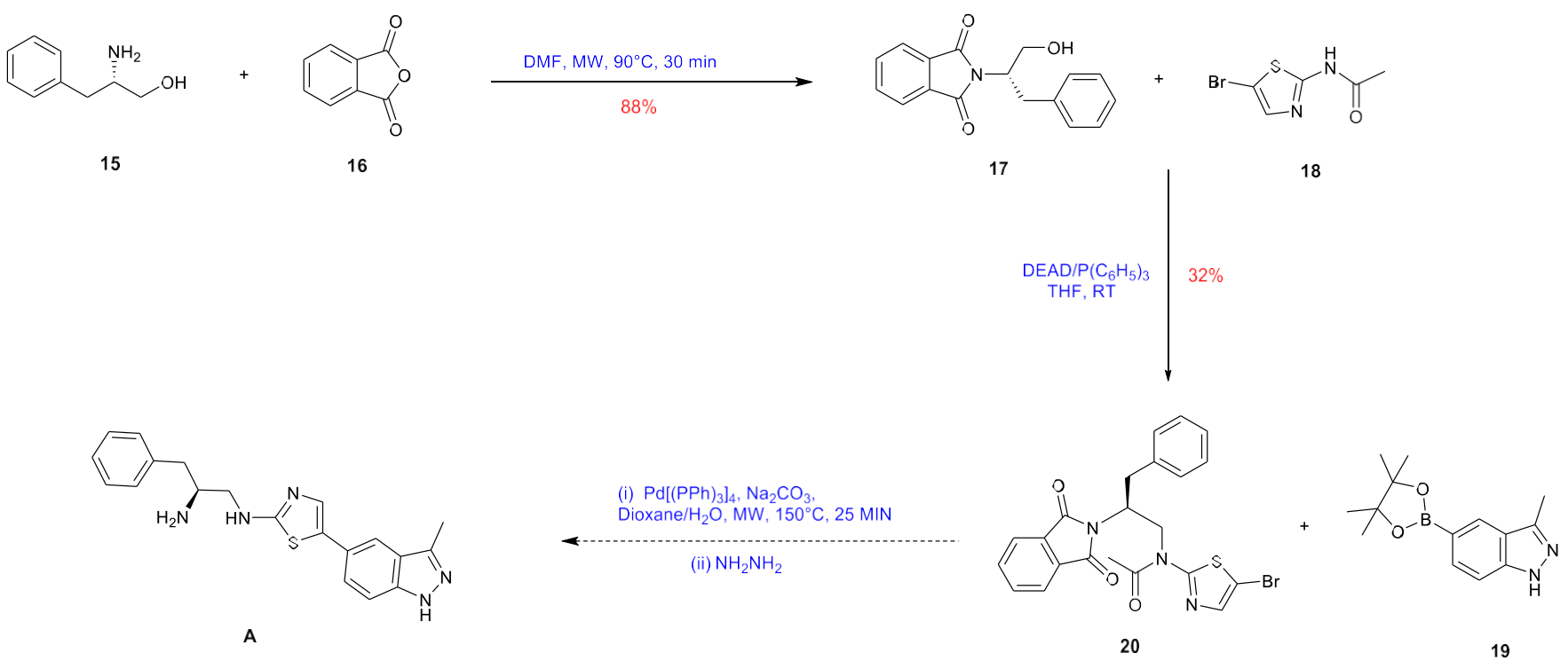

Scheme 3: Synthetic pathway to compound A

14.1 – Cyclocondensation Reaction

The first step in the synthesis of compound A **(scheme 3)** was a cyclocondensation reaction between phthalic anhydride and a tertiary amine to elicit a phthalimide compound **17 scheme 4**. The cyclocondensation reactions for phthalimides occurs over three stages: 1 – nucleophilic attack, 2 - proton transfer, and 3 - dehydration between the o-phthalaldehyde and an amine, resulting in the formation of a phthalimide ring.[31] The first nucleophilic attack stage occurs between the amine **15**, where it attacks the carbonyl carbon of the phthalic anhydride to form an unstable tetrahedral intermediate.[31] This is followed by an intramolecular proton transfer to an adjacent oxygen to form an amide.[31] The reaction concludes with a water molecule being eliminated, forming the imide bond and completing the ring to give compound **17**.[31.] When conducted, this reaction worked well, achieving a high yield similar to the literature. Characterization via liquid chromatography mass spectrometry (LC-MS) provided convincing data consistent with the literature.

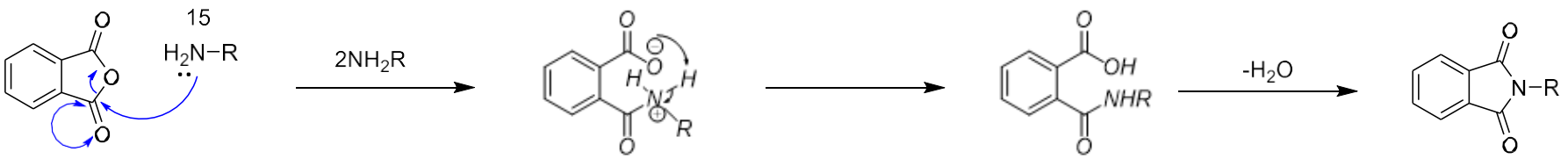

Scheme 4: Mechanism of addition/elimination to yield compound 17.

14.2 Mitsunobu Reaction

The second step of this reaction scheme involved a Mitsunobu reaction between compounds **17** and **18** in the presence of PPh_3 and DEAD **Scheme 5**. Mitsonobu reactions allow for the conversion of primary alcohols into amines when the nucleophile employed is acidic enough to protonate the DEAD reagent, to prevent competing side reactions.[32] In this case, phthalimide compound 17 is a suitable nitrogen nucleophile. The reaction begins with triphenylphosphine combining with DEAD to generate a phosphonium intermediate (ylide).[32] Once activated, the ylide deprotonates the alcohol, which in turn activates the oxygen as a nucleophile, resulting in nucleophilic attack at the triphenyl phosphonium cation to generate a stable O-P bond. Finally, the deprotonated form of the amide **18** displaces triphenylphosphine oxide to form the C-N bond.

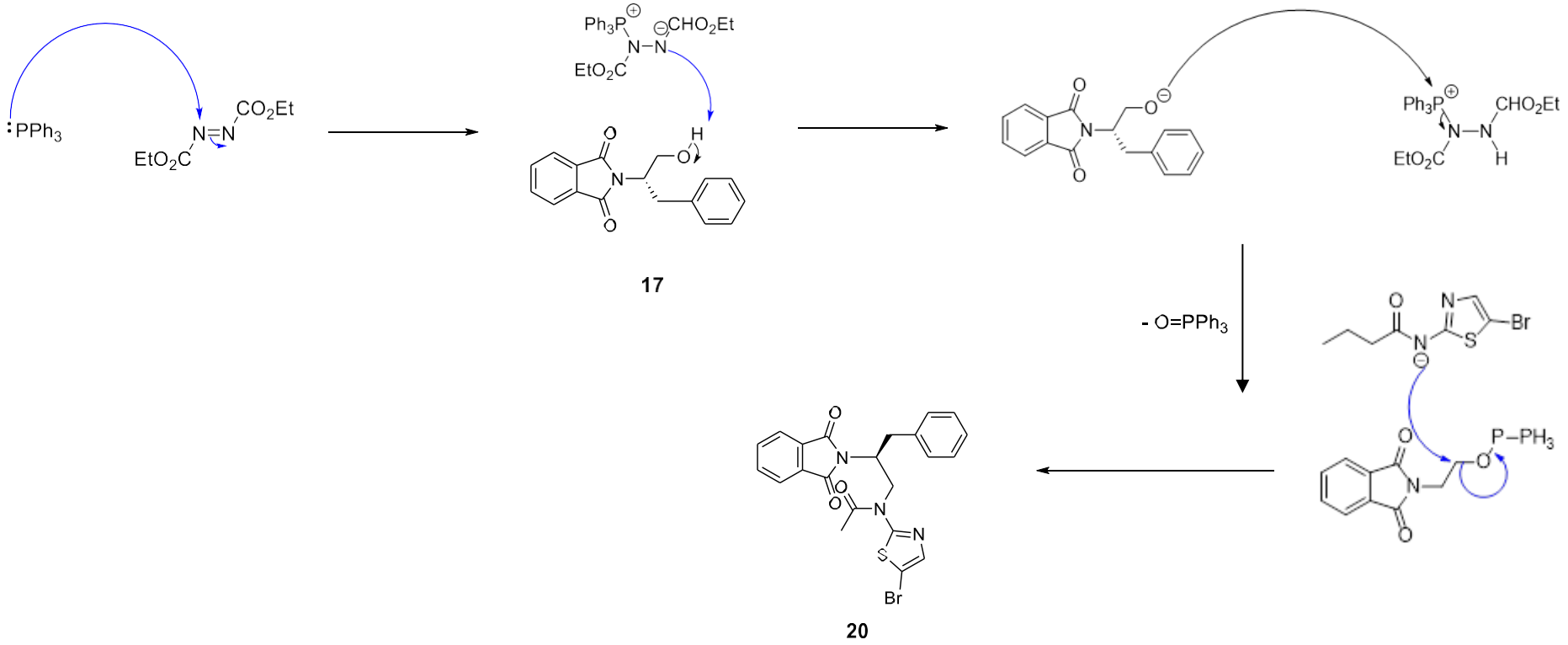

Scheme 5: Mitsunobu reaction mechanism

Unfortunately, we were unable to drive the reaction to completion, resulting in unreacted DEAD, which we were unable to remove and thus obtain a final pure yield of the product. This reaction was repeated multiple times under different temperatures and catalytic quantities, but none of such conditions were able to drive the reaction to completion. In addition, purification was done under normal phase column chromatography, but this was unfruitful due to DEAD and compound **20** having similar retention factor values. High-performance liquid chromatography (HPLC) was used to try and remove the DEAD impurity, but this was not possible as DEAD could not be detected under ultraviolet light (UV), so separation was not possible. Future attempts would involve replacing DEAD with a similar reagent but with a different polarity to the final product, so that separation, despite being a small quantity, would be possible. An example of this would be the Tsunoda reagent.

14.3 Suzuki-Miyaura Borylation

Suzuki-Miyaura borylation reactions are commonly found in organic chemistry as they are used to cross-couple aryl halides to B_2pin_2 to form boronic ester **19**.[33] In this case, it was achieved by reacting 5-bromo-3-methyl-1H-indazole with bis(pinacolato)diboron with a Pd catalyst scheme 6. The Miyaura borylation is composed of four fundamental steps with dppf is the ligand: oxidative addition, ligand exchange, transmetallation & reductive elimination.[33] Starting with oxidative addition, the aryl halide couples onto the Pd^0 complex to give a Pd^{II} intermediate. Ligand exchange follows when potassium acetate substitutes bromide in preparation for transmetallation with B_2pin_2. The final reductive elimination step, where Pd is regenerated and the pinacol boronic ester product is released. The reaction gave a moderate yield of 66% but did not reach completion.

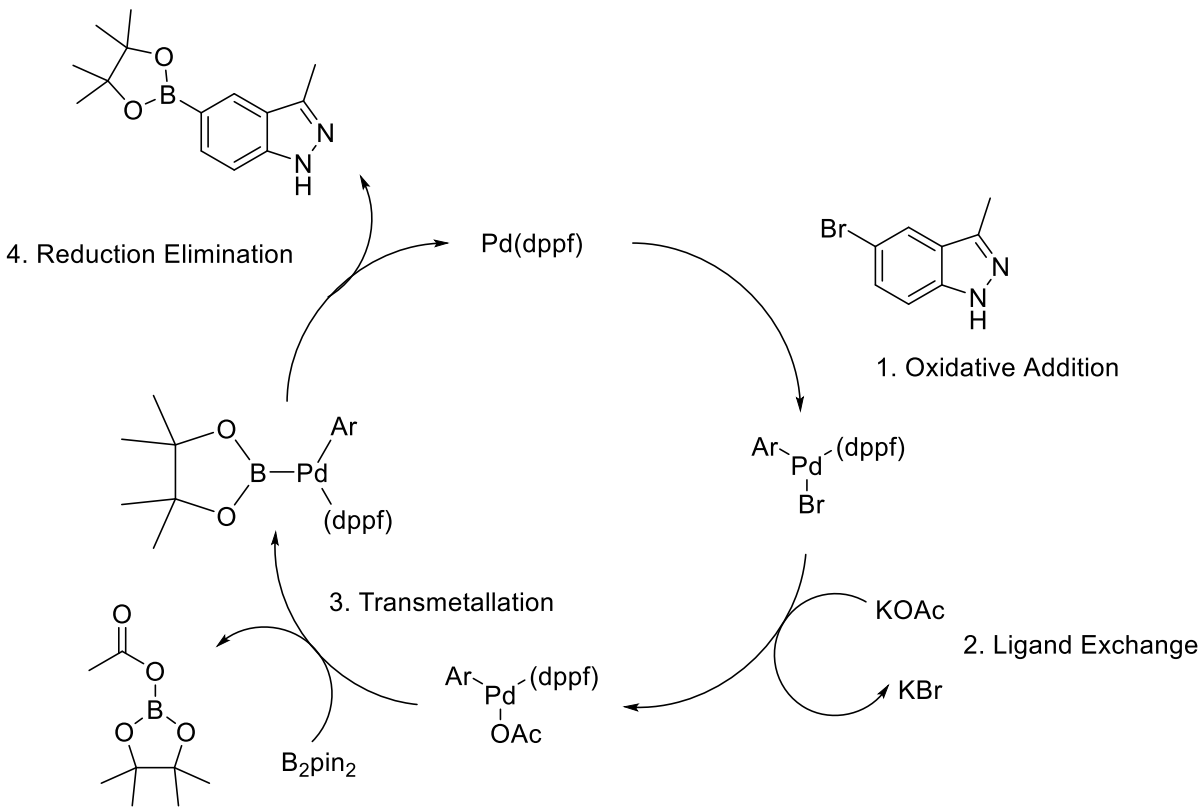

Scheme 6: Miyaura borylation mechanism

14.4 – Suzuki-Miyaura Coupling

The last step of the synthesis was a Suzuki coupling reaction, also known as Suzuki-Miyaura coupling. This reaction did not work well due to DEAD impurities that were carried forward when trying to synthesize compound **20**. As stated previously, both compounds **19** and **20** were difficult to isolate, so essentially two impure compounds were reacted together in the final stage in an attempt to make compound A. The reaction was monitored via TLC, and a ^{1}H NMR spectrum was taken of the crude mixture, but this was inconclusive. In hindsight, failure to synthesize very much of compound **20** was likely because compound **18** is a weak nucleophile that would not have readily reacted with compound **17** to form the desired C-N bond. An alternative approach would be to increase nucleophilicity around the nitrogen atom by reducing steric bulk in the form of an acetyl deprotection on compound **18** before carrying out the Mitsunobu reaction. This could be achieved by reacting compound **18** with an alkyl halide generated from HCl/KOH and EtOH under reflux conditions. This would ultimately generate a more nucleophilic amine that would react better with an alkyl halide generated from compound **17** to give compound **20**. At this stage of the project, however, given the difficulties with isolating compound **20**, it was decided that rather than altering the reaction pathway, we would attempt to make another one of the other *Pf*CLK1 inhibitors.

15.0 - Synthesis of compound B

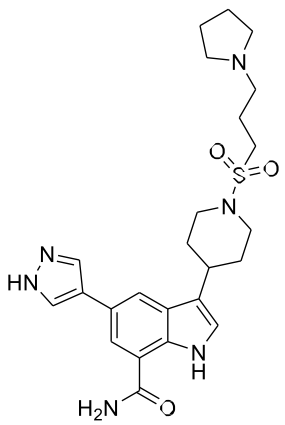

Figure 7 – Compound B

The retrosynthetic disconnections described below were used, primarily, to enable a rigorously regioselective forward synthesis based on well-established chemical transformations **scheme 7**

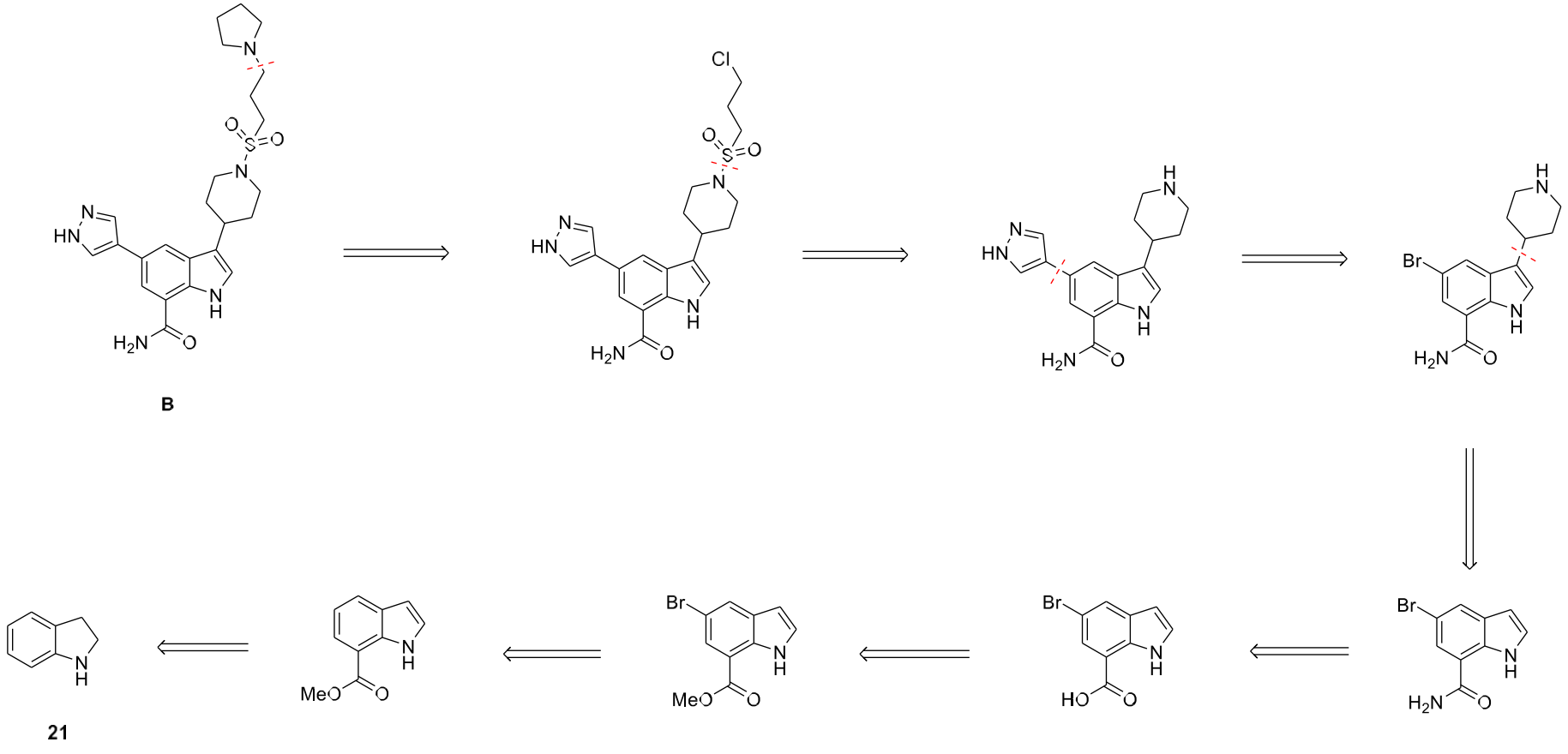

Scheme 7 – Retrosynthesis of compound B

15.1 - Development of the Synthetic Pathway

The synthetic route below was made possible by reading how a similar 3,5-disubstituted indole-7-carboxamide inhibitor had been made for a similar protein kinase IKKβ.[34] Given that compound B was a novel compound, the retrosynthetic analysis was carried out first before carrying out the synthesis to attain the final synthetic product **Scheme 8**. Compound **29** was distinguished with a box mark to mark where the project came to a close. The synthetic pathway began with Boc protection of Indoline to generate a Boc-protected Indoline intermediate 70% yield. The next step involved a C-H activation by directed metalation to generate a methyl ester intermediate **23** in 50% yield. This was achieved by reacting sec-butyllithium, tetraacetylethylenediamine (TMEDA), and methyl chloroformate in anhydrous diethyl ether at -78 °C. The methyl ester intermediate was subsequently reacted with N-Bromosuccinimide at room temperature overnight to give 5-bromoindoline **24** intermediate in 38% yield. This was followed by a Boc deprotection under acidic conditions using trifluoroacetic acid (TFA), giving **25** in a good yield of 82%. Next, 5-bromoindoline **25** was oxidized with manganese dioxide in THF to provide 5-bromoindole **26** in 77% yield. After this, the methyl ester was hydrolyzed to the carboxylic acid using sodium hydroxide in a 1:3 mixture of methanol and water to give compound **27** in 80% yield. An amide coupling reaction was then achieved by coupling together the carboxylic acid and ammonia in methanol using 1-ethyl- 3-(3-dimethylaminopropyl) carbodiimide (EDC) and hydroxybenzotriazole (HOBt) to incorporate the carboxamide at the 7-position of the indole ring to give compound **28** in 60% yield. The last step reached was a Suzuki coupling reaction between **28** and 1H-pyrazole-4- boronic acid, using [1,1'-Bis(diphenylphosphino)ferrocene] palladium (II) dichloride as a catalyst and potassium phosphate as a base in a 1:1 ratio of dioxane and water at reflux for 3 hours. This marks where the reaction sequence came to an end.

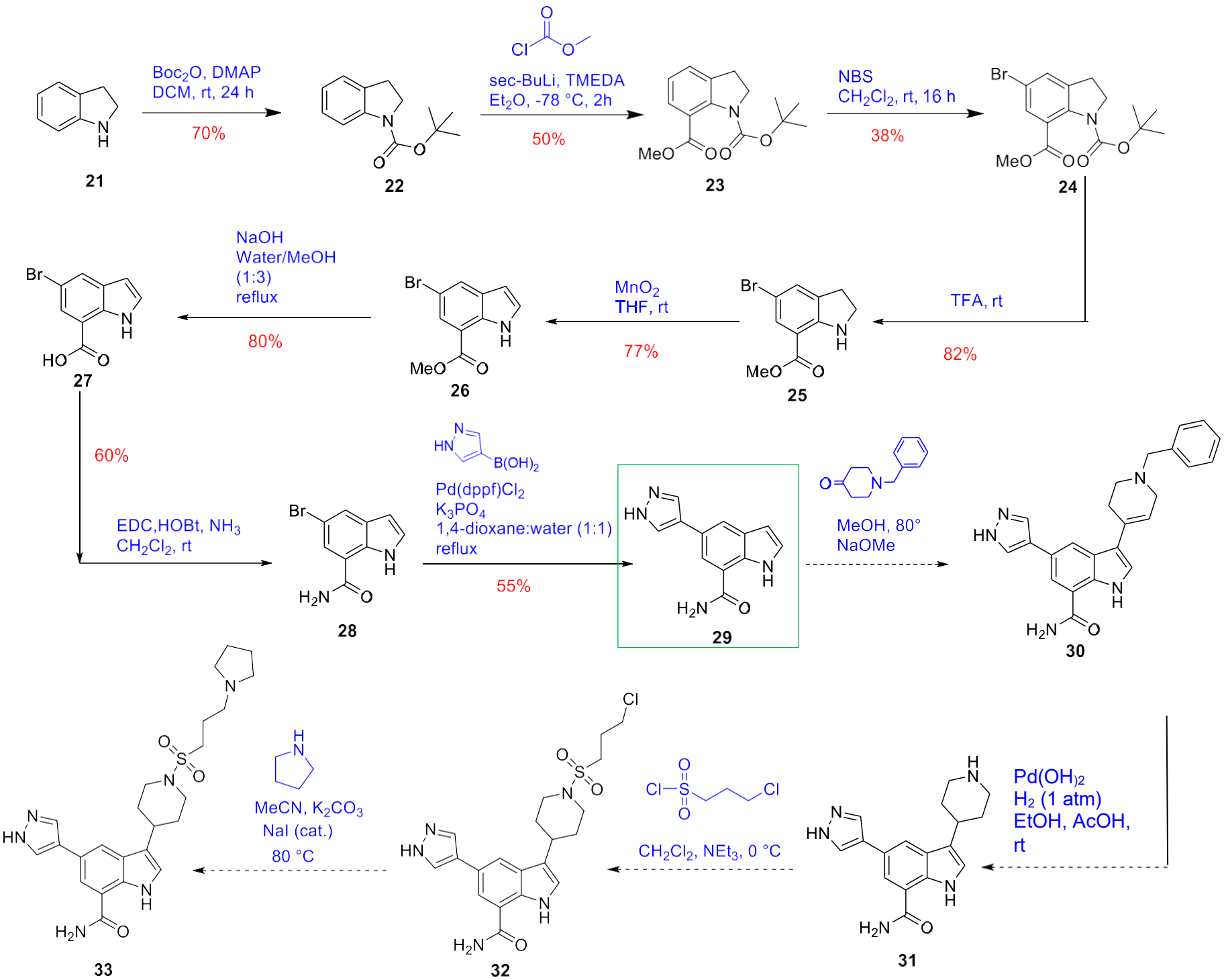

Scheme 8 – Reaction scheme for the synthesis of compound B

15.2 - Adding a Boc Protecting Group

When constructing reaction pathways, functional group protection is a critical component of the synthetic method. There are numerous protecting groups, but the tert-butyloxycarbonyl (Boc) protecting group is the most common in organic synthetic chemistry due to its ease of insertion into organic molecules and subsequent removal from them under acidic or basic conditions. When orthogonally coupled with other protective groups, the Boc protecting group is likewise exceedingly tolerant.

The Boc protecting group is a carbamate group, and one of its key properties is that it is acid-labile but will not react with a base due to high steric hindrance surrounding the carbonyl group.[35] In addition, primary and secondary amines are protected from electrophiles by the bulky nature of the Boc protective group. This is accomplished by removing electron density from nitrogen via the carbonyl group. The reaction begins with DMAP attacking the electrophilic carbon atom of the carbonyl group of Boc anhydride (**scheme 9)**. Next, a lone pair of electrons on compound **21** attacks the recently generated Boc-pyridinium intermediate's electrophilic carbon atom; regenerating DMAP as a catalyst in the reaction mixture. Finally, deprotonation by tert-butyl carbonate anion forms the desired Boc protected Indoline **22**.

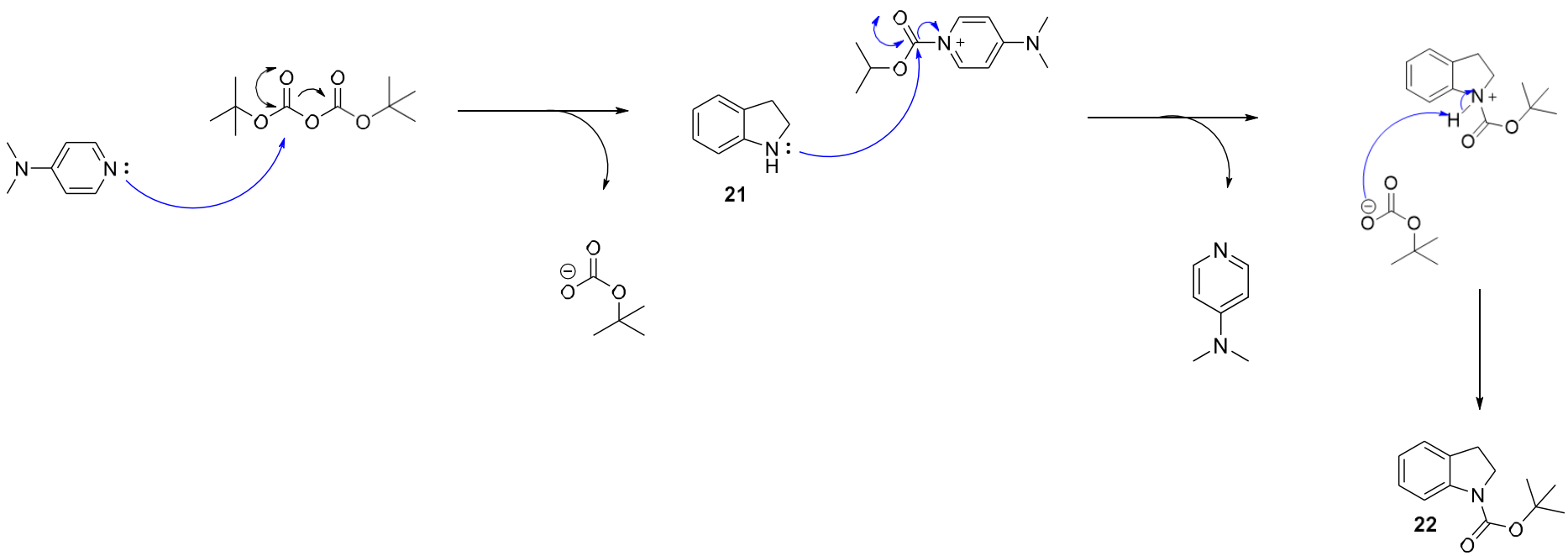

Scheme 9 – Mechanism illustrating Indoline boc deprotection.[35]

Upon synthesizing and purifying the Boc-protected indole **22**, it appeared that the aromatic proton attached to C-7 adjacent to the Boc protecting group was not visible under NMR spectroscopy at 25°C (Figure 8). One rationale for this phenomenon would be that the Boc group was rotating slowly around the N-C bond at 25°C and this was close to the coalescence temperature for this signal. A variable temperature experiment was conducted at 80°C (Figure 9). Increased temperature allowed for rapid interconversion of the Boc rotamers on the NMR timescale so that an average spectrum of the rotamers in (Figure 10) is observed.

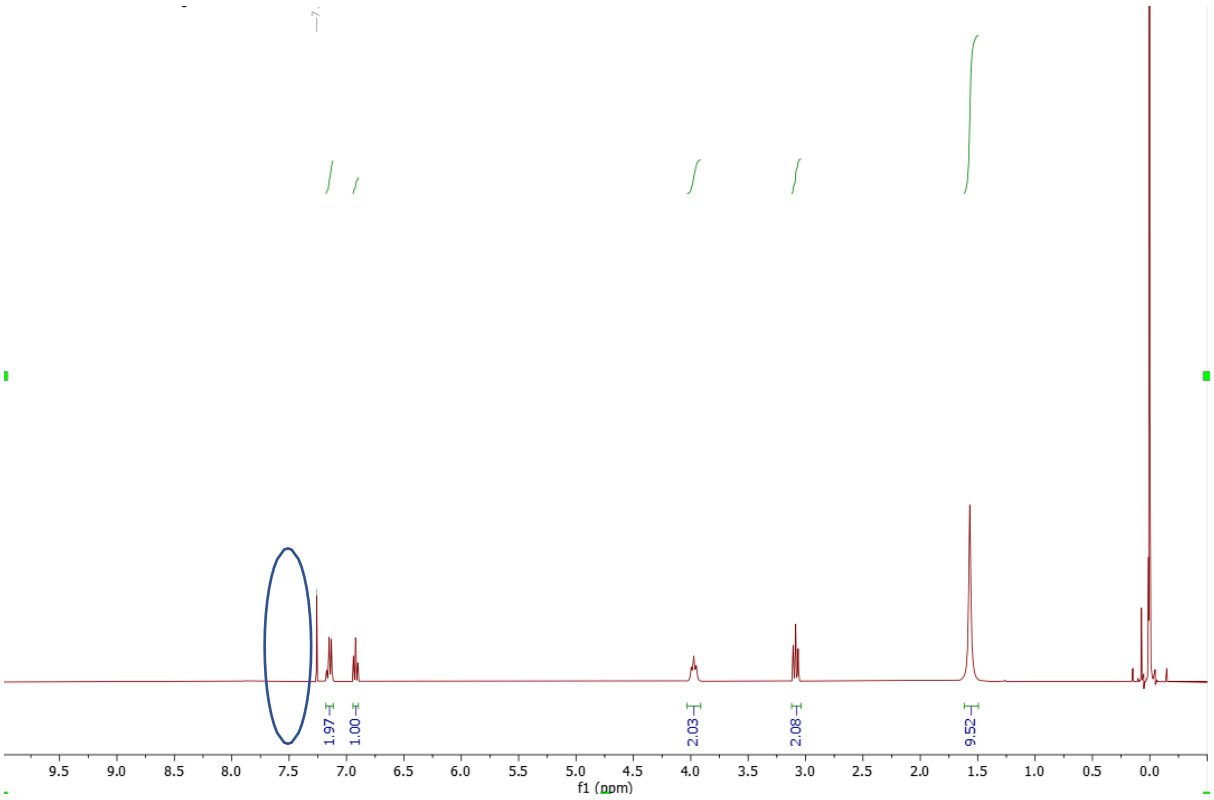

Figure 8 – ^{1}H-NMR experiment at 25 °C

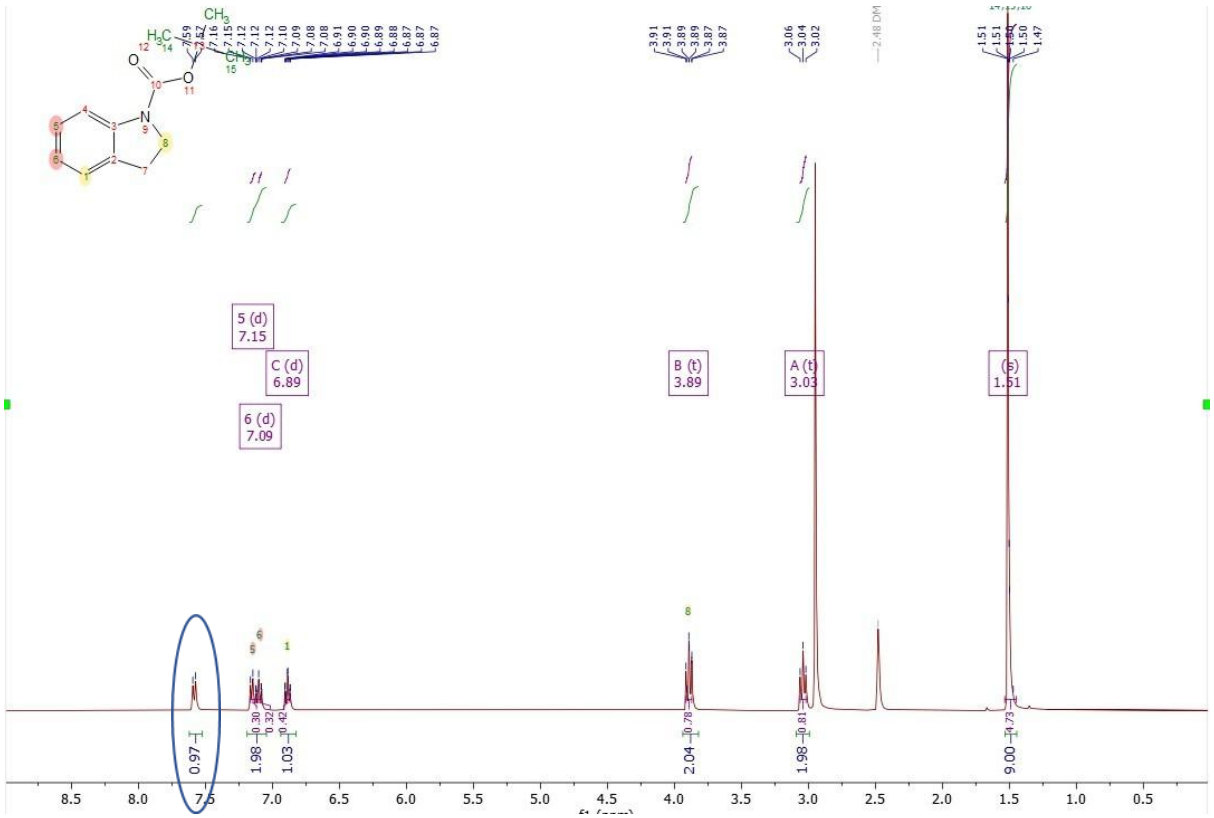

Figure 9 – Variable temperature experiment at 80 °C showing missing peaks

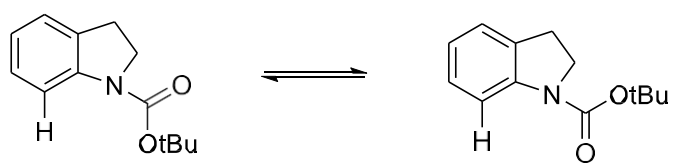

Figure 10 – compound 22 Boc rotamers

15.3 - C-H bond cleavage via directed metalation

Carbon-hydrogen (C-H) bond activation processes refer to the site-selective functionalization of carbon-hydrogen bonds. This functionalization is commonly defined by the replacement of the C-H bond with a new carbon-carbon bond, carbon-oxygen bond, or carbon-nitrogen bond, though other atoms can be used. The most useful C-H activation reactions are those in which site selectivity is governed by a directing group, such as a directed metalation reaction. Directed metalation reactions are a form of substitution reaction in which electrophiles only react in the ortho-position with respect to the directing metalation group (DMG), hence site selectivity.[36] A Lewis basic group is often the guiding metalation group. It can make coordinating contacts with an alkylithium reagent, like a Lewis acid lithium cation. Unlike activating groups, directed metalation groups have no effect on the reactivity of the C-H bond itself. Metalation followed by quenching with an electrophile achieves the desired reaction's regioselectivity, which is preferred over generic electrophilic substitution methods, which would otherwise result in a combination of ortho- and para-products. Because DMGs must coordinate with alkylithium reagents by definition, their presence, that is, the presence of a heteroatom in the DMG, is required for the establishment of a complex-induced proximity effect, which results in the preferential cleavage of one C-H bond over another.

The previously mentioned requirements indicate that the Boc protecting group on the Indoline ring was a good directing group for the selective functionalization of the C-H bond at position 7 of the Indoline ring due to its ortho positioning. The carbonyl carbon atom is normally thought of as a Lewis acid because it attracts electrons. However, the oxygen atom in the carbonyl bond is nucleophilic, so it can act as the Lewis base moiety needed to meet the criteria as a directed metalation group in this case. Sec-butyllithium was used for the project because directed metalation reactions need strong alkylithium reagents to work. Sec-butyllithium is a solvated aggregate with an extremely polarized carbon-lithium σ-bond. For this study, a commercial sample of 1.4 M sec-butyllithium in cyclohexane was utilized; sec-butyllithium exists as a tetramer in cyclohexane. This tetramer arrangement reduced the possible interaction between sec-butyllithium and the starting reagent; hence, a polar aprotic solvent like diethyl ether was used to dissociate the aggregates. TMEDA was also used as a bidentate ligand to break up the sec-butyllithium aggregates even more by turning the tetramers into dimers and monomers Scheme 10 below shows the directed metalation of boc-protected Indoline with methyl chloroformate in the presence of TMEDA and sec-butyllithium. The reaction begins with adding sec-butyllithium and TMEDA, resulting in the boc-directed deprotonation and lithiation at C-7. The lithiated intermediate is then quenched with the methyl chloroformate electrophile to form the final 7- substituted Indoline product **23.**

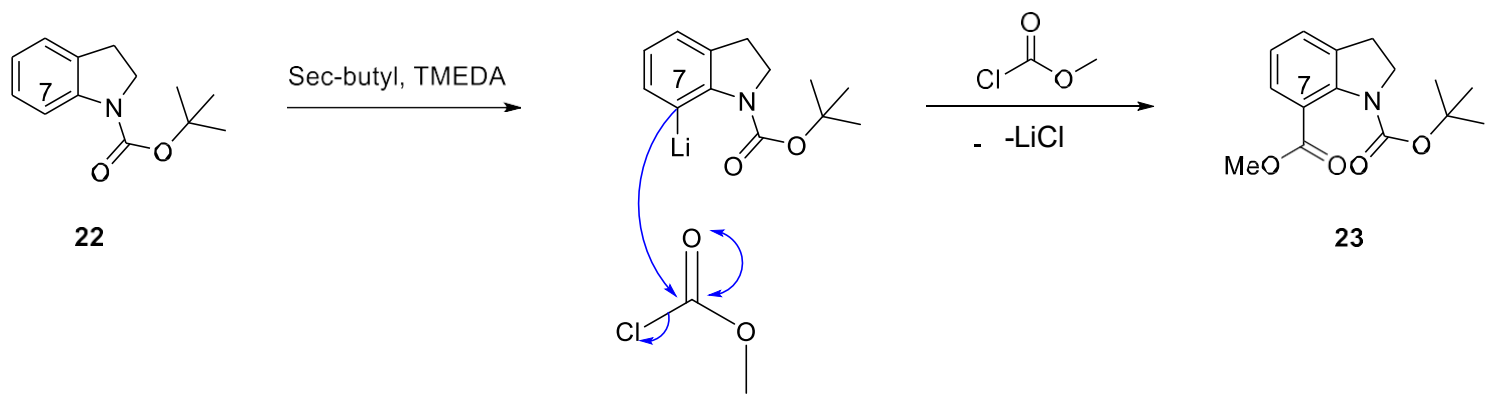

Scheme 10. Mechanism of C-H activation on the indole aryl ring with TMEDA and *sec*-butyllithium.

15.4 - Indole bromination with *N-Bromosuccinimide*

Since carbon-bromine bonds are important precursors for many essential transformations, bromination reactions are commonly found in the pharmaceutical and agrochemical industries. An example of such transformations would be the Suzuki-Miyaura cross-coupling reaction that forms new C-C bonds.

Numerous reagents can be used in bromination processes, from *N*-Bromo succinimide (NBS) to elemental bromine. The latter, however, is avoided in most cases due to its strong corrosive and toxic qualities. In both academia and industry, NBS is a commonly used source of elemental bromine for these transformations due to its ability to facilitate high-yielding reaction outcomes.

In this case, the brominated product is obtained via an electrophilic aromatic substitution between NBS and the benzene segment of Indoline. Due to resonance stabilization, benzene rings are highly susceptible to these kinds of transformations. In this case, the presence of an electron-withdrawing, meta-directing group at the C-7 position reduces electron density in the neighboring ortho position more than in the further away meta; making the meta position more electron dense and the reaction regioselective to the C-5 position. In addition, electrophilic addition at the C-6 ortho position would be unfavorable due to impossible pentavalent resonance structures schethe me 11.

The reaction begins with the benzene segment of the Indoline ring attacking NBS in the mechanism. As this step breaks aromaticity and produces the carbocation intermediates shown in **scheme 11**, this stage of the reaction determines the reaction's rate. Subsequently, the C-H bond cleaves, resulting in the formation of a new C-Br bond and the restoration of the π-bond aromaticity.,

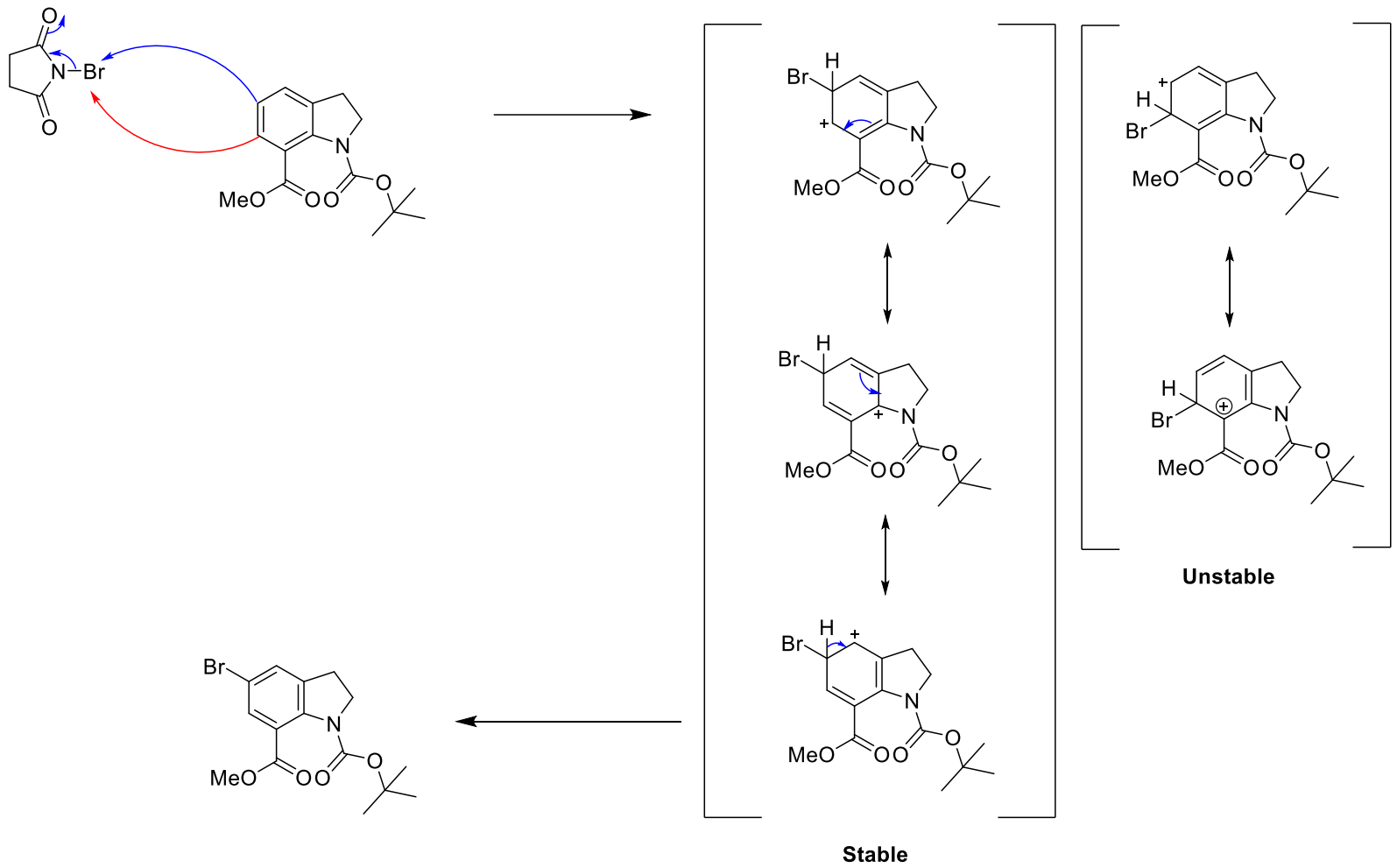

Scheme 11. Mechanism for the bromination reaction on the Indoline

15.5 - Boc deprotection with trifluoracetic acid

The removal of the Boc group is another common reaction within organic chemistry and can be achieved in the presence of acids (TFA), bases (sodium ethoxide in ethanol), or thermolysis, which involves heating the compound to a high enough temperature, causing the Boc group to detach. In the case of scheme 12, TFA acid was employed as a suitable acid. The reaction begins with protonation at the carbonyl oxygen of the Boc group to form an unstable oxocarbenium cation.[37] This rapidly fragments into a stabilized tertiary cation due to inductive effects and is finally deprotonated to form gaseous isobutene.[38] At the same time, the fragmented carbamate can undergo decarboxylation to release the desired free amine compound 25, carbon dioxide, and the regenerated acidic proton.

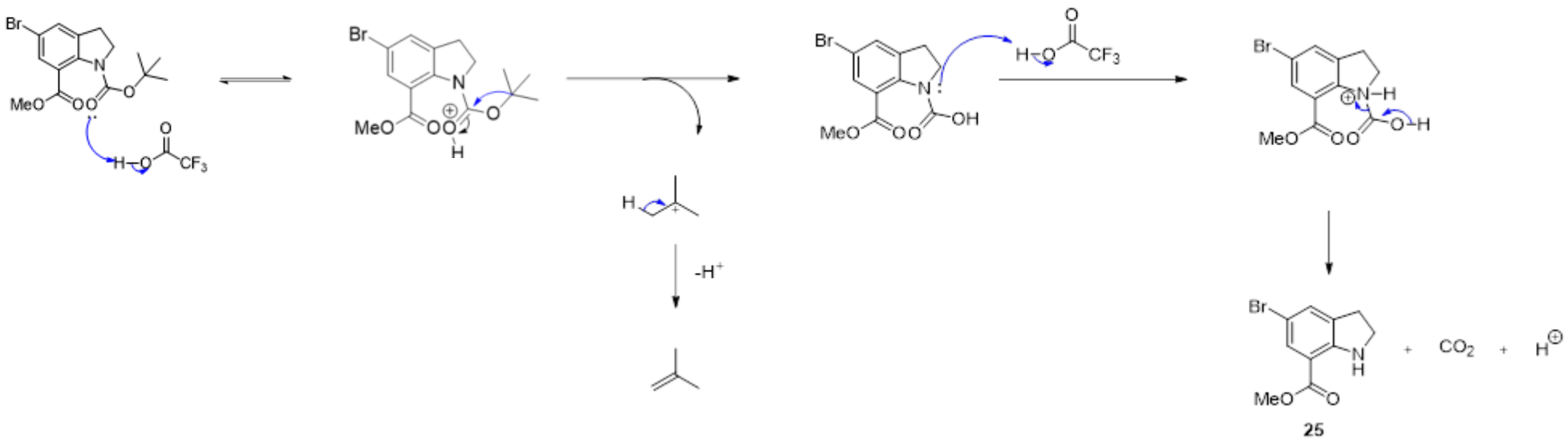

Scheme 12. Mechanism illustrating TFA Boc deprotection.[37]

15.6 – Indoline dehydrogenation

The indole ring is the most significant component of the target molecule in the synthetic pathway. After deprotection with TFA, the Indoline ring needed to be oxidized to produce the essential indole PharmaCore. Within organic synthetic chemistry, dehydrogenation reactions are one of the most common and versatile classes of reactions. Multiple catalysts could have been employed as oxidizing agents for this reaction like palladium dichloride or gold trichloride, but due to its availability manganese dioxide which is a common mentioned reagent in the literature was used. The mechanism of reaction can be broken down into five stages; 1 - adsorption, 2 - electron transfer, 3 – dehydrogenation, 4 - desorption and 5 tautomerization **scheme 13**. Step one involves the Indoline being adsorbed onto the surface of the manganese dioxide. The manganese(IV) dioxide accepts electrons from Indoline. This is followed by a hydrogen atom at C2 being cleaved. Before or after desorption tautomerization results in the aromatization of the Indoline ring to give an indole ring and the final reduced manganese(II) oxide. The final resulting indole ring is stabilized by aromaticity, making it more stable and less reactive in comparison to Indoline.

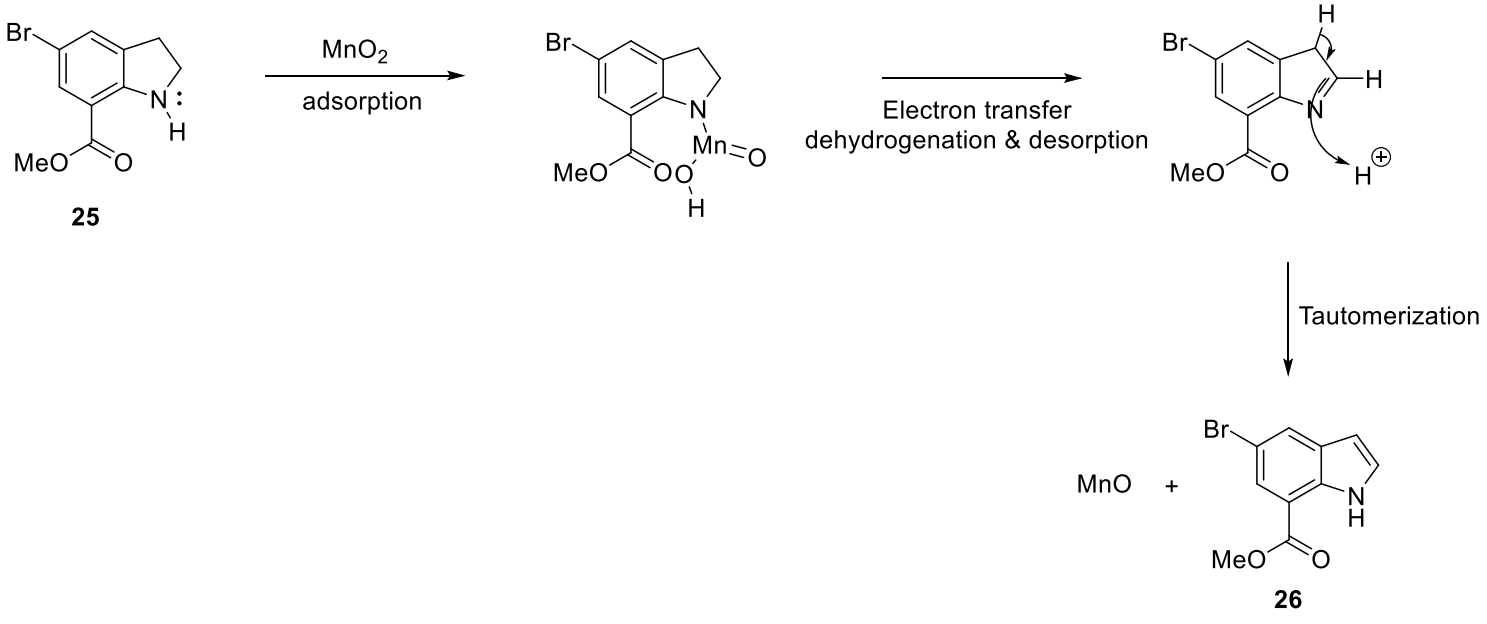

Scheme 13 - Mechanism of aromatization oxidation using manganese dioxide.

15.7 - Methyl ester hydrolysis

Organic synthetic chemistry routinely involves ester hydrolysis reactions Scheme 14. Ester hydrolysis reactions can be broken down into three stages: 1 – nucleophilic addition, 1 – elimination, and 3 – deportation of the carboxylic acid. In the first stage of base-catalyzed ester hydrolysis the nucleophilic hydroxyl group attacks the carbonyl carbon, pushing electrons on the carbonyl oxygen. This is swiftly followed by the reformation of the carbon and oxygen double bond and the elimination of the ester group. In the final stage, the ester group deprotonates the acidic carboxylic acid, leaving behind compound 27.

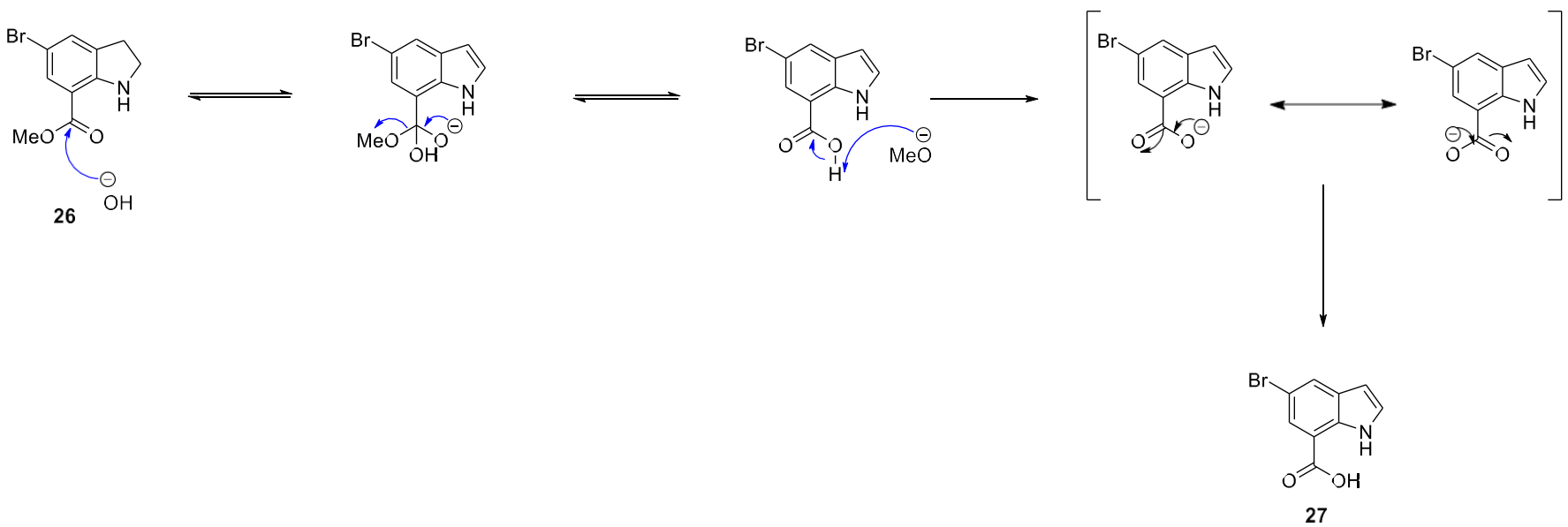

Scheme 14. Mechanism of ester hydrolysis to the carboxylic acid.

15.8 - Amide coupling

Amide coupling is a chemical reaction that forms amide bonds N-C. The amide coupling reaction is crucial in the organic synthesis of many proteins and pharmaceutical drugs. This reaction is typically achieved by the condensation of a carboxylic acid and amine in the presence of a coupling reagent, in this case EDC (1-ethyl-3-(3-dimethylaminopropyl)carbodiimide). The reaction begins with the coupling reagent EDC activating the carboxylic acid as the carboxylic acid on its own is not reactive enough to interact with the amine. Once achieved the amine acts as a nucleophile, attacking the carbonyl carbon of the activated carboxylic acid, resulting in the formation of the new amide (N-C) bond. EDC fragment is also cleaved in the process **scheme 15**.

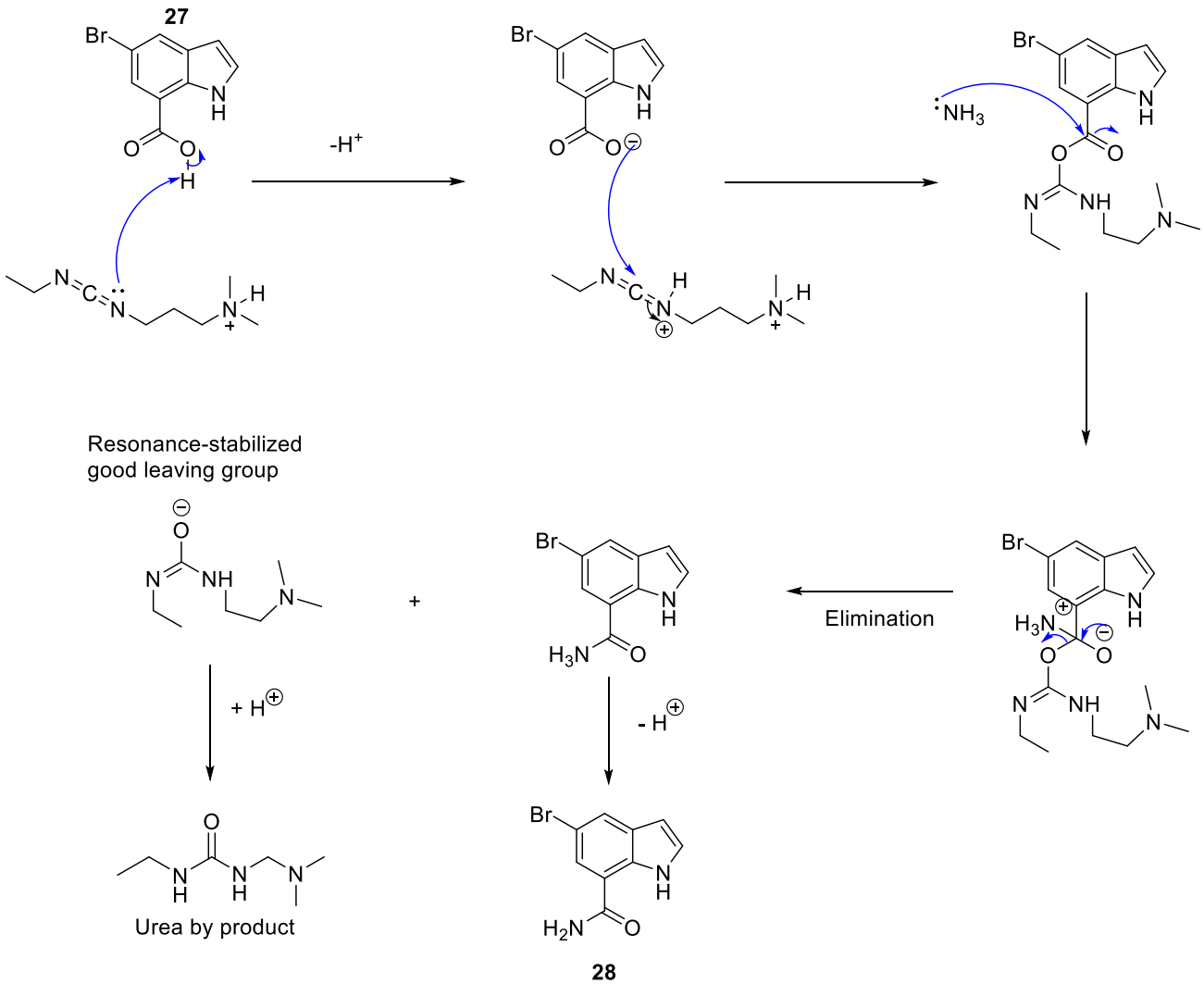

Scheme 15 - Mechanism of amide coupling using EDC and HOBt

15.9 – Suzuki-Mayuri cross coupling

The Suzuki-Miyaura coupling is a palladium-catalyzed cross-coupling reaction used to form carbon-carbon bonds. This reaction involves the coupling of organohalides with organoboron in the presence of a base to form more complex organic compounds. The reaction proceeds through a catalytic cycle and can be observed in four stages: 1 – oxidative addition, 2- ligand exchange, 3- transmetallation and reductive elimination.

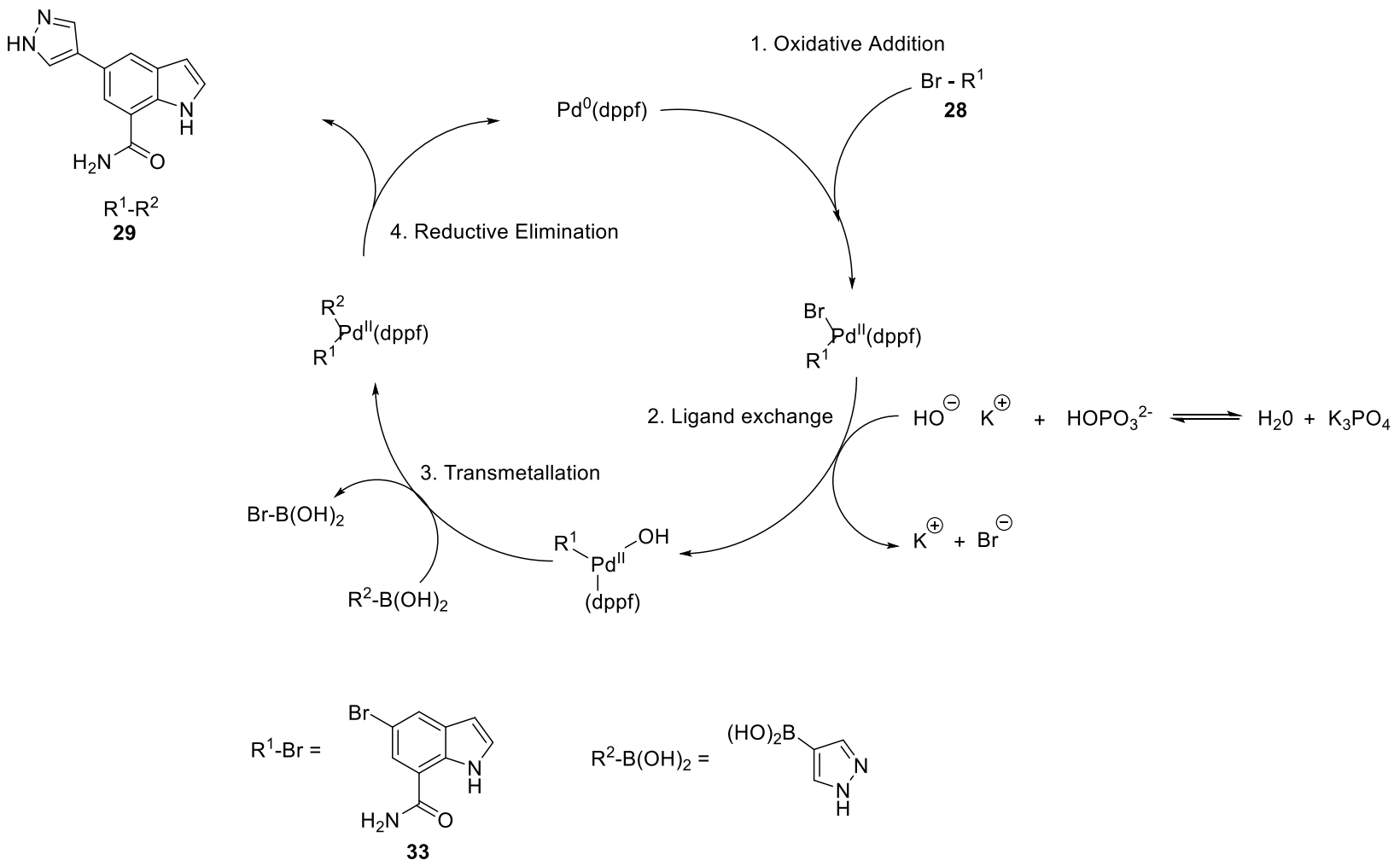

Scheme 16 - Catalytic cycle showing Suzuki coupling[39]

The Suzuki reaction can be influenced by the ligand that is bound to the palladium catalyst. The Pd(dppf) catalyst was employed in this project for several purposes. Firstly, compared to its more commonly used counterpart, Pd $(PPh_3)_4$ (tetrakis(triphenylphosphine) palladium), it shows superior air and moisture stability. Second, the phenyl and ferrocene ligands' bulkiness and steric effects, along with the large P-Pd-P bite angle the final reductive elimination step is accelerated.

16.0 - Conclusion and Future work

The recent rise of artemisinin-resistant malaria parasites poses a serious threat to the control of malaria, and thus more active antimalarial treatment is urgently required. Recent studies have identified the cyclin-dependent protein kinases family (*Pf*CLK1-4) as a novel and therapeutic target to treat malaria. The successful validation of *Pf*CLK3 as a potential therapeutic target for malaria inspired the study of a similar protein kinase of the same family, *Pf*CLK1. This project, however, remains in its initial stages. If it can be proven that inhibitors of *Pf*CLK1 can prove efficacious across both the sexual and asexual stages of the parasite lifecycle, then it is likely that these inhibitors will pave the way for the next generation of antimalarial drugs.

Future work will include attempting to synthesize all four of the *Pf*CLK1 inhibitors from the high-throughput screening. Once compounds have been synthesized, structure-activity relationship studies using molecular docking will be conducted to make suitable analogues. Analogues could then be subjected to biological testing to establish inhibitory potency (TR-FRET) and in vivo antiparasitic activity (3D7 *F*alciparum parasites). Successful analogues could then be optimized into covalent binders via the addition of suitable lysine-targeting warheads. While this project is still in its preliminary stages, it can expand our understanding of the role of P*f*CLK1 in the malaria lifecycle and validate it as a new therapeutic target.

17.0 Experimental

17.1 - Experimental Procedures

Chemicals and solvents were purchased from standard suppliers and used without additional purification. When necessary, glassware was dried in the oven overnight and left to cool before usage in a desiccator. Anhydrous solvents (THF, DCM, and Et2O) were obtained from the School of Chemistry solvent purification system (SPS – Thermo Fisher Scientific UK), and solvents were transferred by syringe under a nitrogen atmosphere into their respective reaction vessel. All reactions in an inert or dry atmosphere were done under a nitrogen blanket.

Thin-layer chromatography (TLC) - was performed using aluminum plates precoated with silica gel (0.25 mm (about 0.01 in), 60 Å pore-size) impregnated with a fluorescent indicator (254 nm). Visualization on TLC was achieved with UV light (254 nm).

Flash column chromatography (FCC) - was undertaken manually on silica gel (400-630 mesh).

Proton nuclear magnetic resonance spectra (1H NMR) - It was recorded on an AVANCE III 400 Bruker (400 MHz). Proton chemical shifts are expressed in parts per million (ppm, δ scale) and are referenced to residual protium in the NMR solvent (CDCl3, δ 7.26; CD3OD, δ 3.31; and DMSO-d6, δ 2.50). The following abbreviations were used to describe peak patterns when appropriate: br = broad, s = singlet, d = doublet, t = triplet, q = quadruplet, sept = septet, and m = multiplet. The coupling constants, J, were reported in hertz units (Hz). Carbon-13 nuclear magnetic resonance spectroscopy

Carbon 13 Nuclei Magnetic Resonance (13C NMR) - was recorded on AVANCE III 400 Bruker (101 MHz) and was fully decoupled by broad band decoupling. Chemical shifts were reported in ppm referenced to the center line of a triplet at 77.0, 49.0, and 39.5 ppm of CDCl3, CD3OD, and DMSO-d6.

Low resolution mass spectrometry (LRMS) - was performed on a Thermo Scientific LCQ Fleet quadrupole mass spectrometer using electrospray ionization in positive mode (ESI+), employing a 150 mm (about 5.91 in) x 4 mm (about 0.16 in) C18 column (Dr. Maisch Reprosil Gold).

17.2- Experimental Methods

17.2.1 -(S)-2-(1-hydroxy-3-phenylpropan-2-yl)isoindoline-1,3-dione

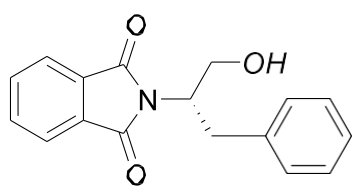

17

Isobenzofuran-1,3-dione (1.10 g, 7.44 mmol, 1 equiv.) and (S)-2-amino-3-phenylpropan-1-ol (1.12 g, 7.44 mmol, 1 equiv.) were charged into a 20 mL microwave tube along with dioxane 10 mL and sealed. The microwave tube was heated at 90 °C for 30 mins in a CEM microwave reactor. Dioxane was evaporated under reduced pressure to give the crude residue. Purification was carried out by flash column chromatography Pet Ether-EtOAc (4:6) to give (*S*)-2-(1-Hydroxy-3-phenylpropan-2-yl) isoindoline-1,3-dione (1.85g, 88% yield). M.p. 117 – 119 °C; Rf = 0.3 (Ethyl acetate in PET ether 40-60 °C).[40] ^{1}H NMR (400 MHz, CDCl3) δ: 7.78 (m, 2H), 7.68 (m, 2H), 7.22 (s, 5H), 4.64 (m, 1H), 4.07 (tdd, J = 8.1, 7.2, 3.6 Hz, 1H), 3.94 (m, 2H), 3.21 (dd, J = 11.9, 3.6 Hz, 1H), 1.6 (m, 1H). ^{13}C NMR (101 MHz, $CDCl_3$) δ: ^{13}C NMR (101 MHz, CDCl3) δ: 168.5, 137.2, 134.1, 131.5, 129.1, 128.3, 126.4, 123.1, 62.7, 60.2, 55.2, 34.7, 21.1, 14.1;[40]

LCMS m/z calcd for $C_{17}H_{16}NO_3$ [M+H]+ 282.1052 found 282.1064 (Δ = 2.1 ppm).

Lit-[α]D20 = -129 (c = 0.9 g/100mL, $CHCl_3$

17.2.2 - 1-Boc-indole

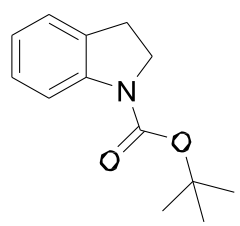

22

Indoline (20.00 g, 167.8 mmol, 1.0 equiv) and 4-dimethylaminopyridine (2.50 g, 16.78 mmol, 0.1 equiv) were dissolved in dichloromethane (500 mL). A solution of di-tert-butyldicarbonate (40.00 g, 185 mmols, 1.1 equiv) in dichloromethane (126 mL) was added dropwise under ice bath conditions. The mixture was stirred at room temperature overnight. Once the reaction had reached completion via TLC analysis, the reaction mixture was washed with brine, dried over magnesium sulphate, and concentrated under reduced pressure. Purification was carried out by flash column chromatography Rf = 0.4 (petroleum ether 40-60: ethyl acetate 97:7) to produce the desired product 1-Boc-indole (25.63 g, 69% yield). M.p. 45-48 °C.^{1}H NMR (400 MHz, CDCl3) δ**:** 1.51 (9H, s), 3.04 (2H, t, J=8.7 Hz), 3.89 (2H, t, J=8.7 Hz), 6.89 (1H, t, J=7.6 Hz), 7.11(2H, m), 7.58 (1H, br, s)

LCMS: m/z (ESI): calcd for C_8H_9N[M+H] 220; found, 220.124.[34]

17.2.3 - (1,1-Dimethylethyl) 7-methyl-2,3-dihydro-1H-indole-1,7-dicarboxylate

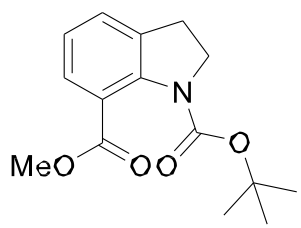

23

1,1-dimethylethyl-2,3-dihydro-1H-indole-1-carboxylate (12.8 g, 58.5 mmols, 1 equiv.) and *N,N,N′,N′*-tetramethyl-1,2-ethanediamine (16.7 ml, 111.2 mmols, 1.9 equiv.) were dissolved in dry diethyl ether (725 mL) and cooled to -78 °C in an acetone and dry ice bath. Sec-butyllithium (1.4 M in cyclohexane, 64.3 mL, 93.6 mmols, 1.6 equiv.) was added dropwise and the reaction allowed to stir at -78 °C for 90 mins. After 90 mins, methylchloromate (19.9 mL, 257 mmols, 4.4 equiv.) was added and the reaction was left to stir at room temperature overnight. The reaction was quenched the next morning with 50 mL of water at -78 °C whilst stirring. The organic layer was then washed with brine to remove excess water and finally fried with MgSO4(s), filtered, and concentrated in vacuo. The crude product was purified by manual column chromatography, Rf – 0.6 (petroleum ether: ethyl acetate, 10:90) to produce the gummy yellow solid (1,1-Dimethylethyl) 7-methyl-2,3-dihydro-1H-indole-1,7-dicarboxylate (7.6 g, 46%); ^{1}H NMR (400 MHz,CDCl3) δppm; 1.44 (s, 9 H), 3.06 (t, J=8.2 Hz, 2 H) 3.69(s, 3 H), 4.02 (t, J=8.3 Hz, 2 H), 7.06 (t, J=7.5 Hz, 1 H), 7.35 (d, J=7.5 Hz, 1 H), 7.39 (dd, J=7.4, 1.1 Hz, 1 H)

LCMS: m/z (ESI): calcd for $C_{13}H_{17}NO_2$[M+H] 278.32; found, 278.4550[34]

17.2.4 - 1-(1,1-Dimethylethyl)7-methyl-5-bromo-2,3-dihydro-1H-indole-1,7-dicarboxylate

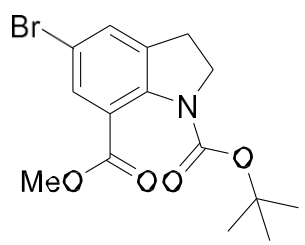

24

1-(1,1-Dimethylethyl) 7-methyl-2,3-dihydro-1H-indole-1,7-dicarboxylate (6.2 g, 22.4 mmol, 1.0 equiv) and N-bromosuccinimide (4.0 g, 22.4.mmol, 1.5 equiv.) were dissolved in dichloromethane (200 mL) and stirred for 16 hours at room temperature under a nitrogen atmosphere . The reaction mixture was portioned with sodium hydroxide (2M), separated and washed with more sodium hydroxide solution. The organic layers were combined and dried over MgSO4 filtered and the crude product was purified by manual chromatography to yield the desired gummy reds solid 1-(1,1-Dimethylethyl)7-methyl-5-bromo-2,3-dihydro-1H-indole-1,7-dicarboxylate (3.55 g, 44.5%); ^{1}H NMR (400 MHz, CDCl3) δppm 1.51 (s, 9 H) 3.1 (t, J=8.3 Hz, 2 H) 3.70 (s, 3 H) 4.02 (t, J=8.3 Hz, 2 H) 7.46 (s, 1 H) 7.60 (s, 1 H)

MS m/z 356/358 (1:1 ratio) $(M+1)^{+}$3.52 min[34]

17.2.5 - Methyl 5-bromo-2,3-dihydro-1H-indole-7-carboxylate

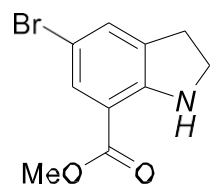

25

1-(1,1-Dimethylethyl)7-methyl-5-bromo-2,3-dihydro-1H-indole-1,7-dicarboxylate (11.54 g, 32.40 mmol, 1.0 equiv.) was dissolved in trifluoracetic acid (62.8 ml) was stirred at room temperature for 16 hours. At this point, 2 M sodium hydroxide solution (30 mL) was added until the aqueous layer reached pH 7. The resulting solution was then extracted with dichloromethane (3 x 10 mL). The organic layer was extracted and dried over MgSO4, filtered, and concentrated in vacuo to yield the desired compound Methyl 5-bromo-2,3-dihydro-1H-indole-7-carboxylate (5.63g, 75%) as a brown solid without the need for purification.[1]H NMR (400 MHz, CDCl3) δppm 2.99 (t, J=8.5 Hz, 2 H) 3.61 (t, J=8.4 Hz, 2 H) 3.78 (s, 3 H) 6.72 (s, 1 H) 7.28 (d, J=1 Hz, 1 H) 7.46 (d, J=2 Hz, 1 H)

MS m/z 256/258 (1:1 ratio) (M+1)+3.32 min.[34]

17.2.6 - Methyl-5-bromo-1H-indole-7-carboxylate

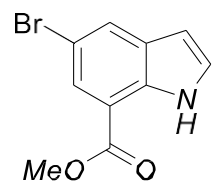

26

Under anhydrous conditions 5-Bromo-1-H-indole-7-carboxylic acid (5.63 g, 21.9 mmol, 1.0 equiv) was dissolved in THF (112 mL). Manganese dioxide (19 g, 219 mmol, 10 equiv.) was added and the mixture was stirred at room temperature overnight. The mixture was then filtered through a pad of celite and concentrated in vacuo. The crude product was finally purified by column chromatography, 0.41 (petroleum ether (40-60): ethyl acetate 70:30. To yield the desired product methyl-5- bromo-1H-indole-7-carboxylate (3.67 g, 77.1 %) as a white solid.[1]H NMR (400 MHz, CD30D) δppm; 3.94 (s,3 H) 6.58 (d, J=3 Hz, 1 H) 7.48 (d,J=3 Hz, 1 H) 7.8 (d, J=2 Hz, 1 H) 8.07 (d, J=1.8 Hz, 1 H) 11.39 (bs, 1 H)

MS m/z 252/254 (1:1 ratio) (M-1) 3.41 min[34]

17.2.7 - 5-Bromo-1H-indole-7-carboxylic acid

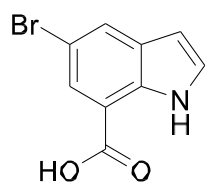

27

5-Bromo-1H-indole-7-carboxylate (3.67 g, 14.50 mmol, 1.0 equiv.) was dissolved in methanol (147 mL) and a solution of sodium hydroxide (1.16 g, 29.0 mmol. 2.0 equiv.) in water (11.6 mL) was added. The reaction was left to heat to reflux for 24 hrs and then acidified using 1 M HCL until a pH of 7 was reached to form a white precipitate. The precipitate was then filtered off and dried under high-vacuum overnight to produce the desired compound 5-bromo-1H- indole-7-carboxylic acid (3.13g, 90%) as beige solid. No further purification was required.

^{1}H NMR (400 MHz, CD30D) δ ppm: 6.53 (d, J= 3.1 Hz, 1H) 7.38 (d, J= 3.2 Hz, 1 H) 7.89 (bs, J=2 Hz, 1H) 7.94 (bs, J=1.8 Hz, 1 H)

LC/MS m/z 238/240 (1:1 ratio) (M-1) 3.41 min.[34]

17.2.8 - 5-Bromo-1H-indole-7-carboxamide

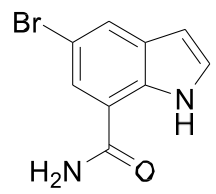

28

5-Bromo-1H-indole-7-carboxylic acid (3.13 g, 13.34 mmol, 1.0 equiv.) was dissolved in dichloromethane (313 mL). EDC (3.06 g, 16.01 mmol, 1.2 equiv.), HOBt (2.16 g, 16.01 mmol, 1.2 equiv.) and NH3 (7.0M in MeOH, 7.5 mL, 53.56 mmol, 4.0 equiv.) were added and left to stir at ambient temperature for 12 hours. After this time, the solvent was evaporated, and the remaining residue was partitioned between ethyl acetate and water. The water layer was extracted with ethyl acetate and the combined organic phase was dried over MgSO4, filtered, and concentrated before purification by manual column chromatography to yield the desired product 5-Bromo-1H-indole-7-carboxamide (1.75 g, 55%) as a white solid.^{1}H NMR (400 MHz, CD30D) δ ppm 1.29 (s, 2H), 6.50,(d, J=2.8 Hz, 1H), 7.38 (d, J=3 Hz, 1) 1H) 7.79 (s, 1H), 7.89(s, 1H)

LC/MS: m/z 240.0 (M+H) 1.95 min[34]

17.2.9 - 5-Pyrazole-1H-indole-7-carboxamide

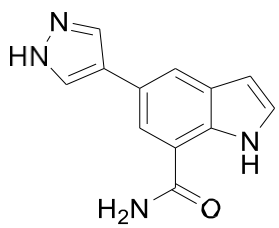

29

5-Bromo-1H-indole-7-carboxamide (1.75 g, 7.73 mmol, 1.0 equiv.), 1-H-pyrazole-4-boronic acid (2.60 g, 22.0 mmol, 3.0 equiv.) and potassium phosphate tribasic (3.11 g, 14.66 mmol, 2.0 equiv.) were dissolved in 1,4-dioxane (36.8 mL) and water (36.8 mL). The reaction was purged under nitrogen gas while stirring for 15 minutes. 1,1′-Bis(diphenylphosphino)ferrocene complex was then added partially whilst mixing and the mixture was left to heat under reflux for 3 hours. The reaction mixture was then cooled to room temperature and then filtered through celite. The filtrate was then partitioned between ethyl acetate and brine. The organic layer was dried over MgSO4(s), filtered, and concentrated before purification, Rf = 0.45 (methanol:dichloromethane:triphenylamine, 8:90:2) by manual column chromatography to yield the desired product (957 mg, 55%). ^{1}H NMR (400 MHz, **CD_3OD)** δ 3.35 (s, 1H), 6.51 (s, 1H), 7.36-8.00 (m, 4H,)

18.0 Appendix

Compound 1 - (S)-2-(1-hydroxy-3-phenylpropan-2-yl)isoindoline-1,3-dione

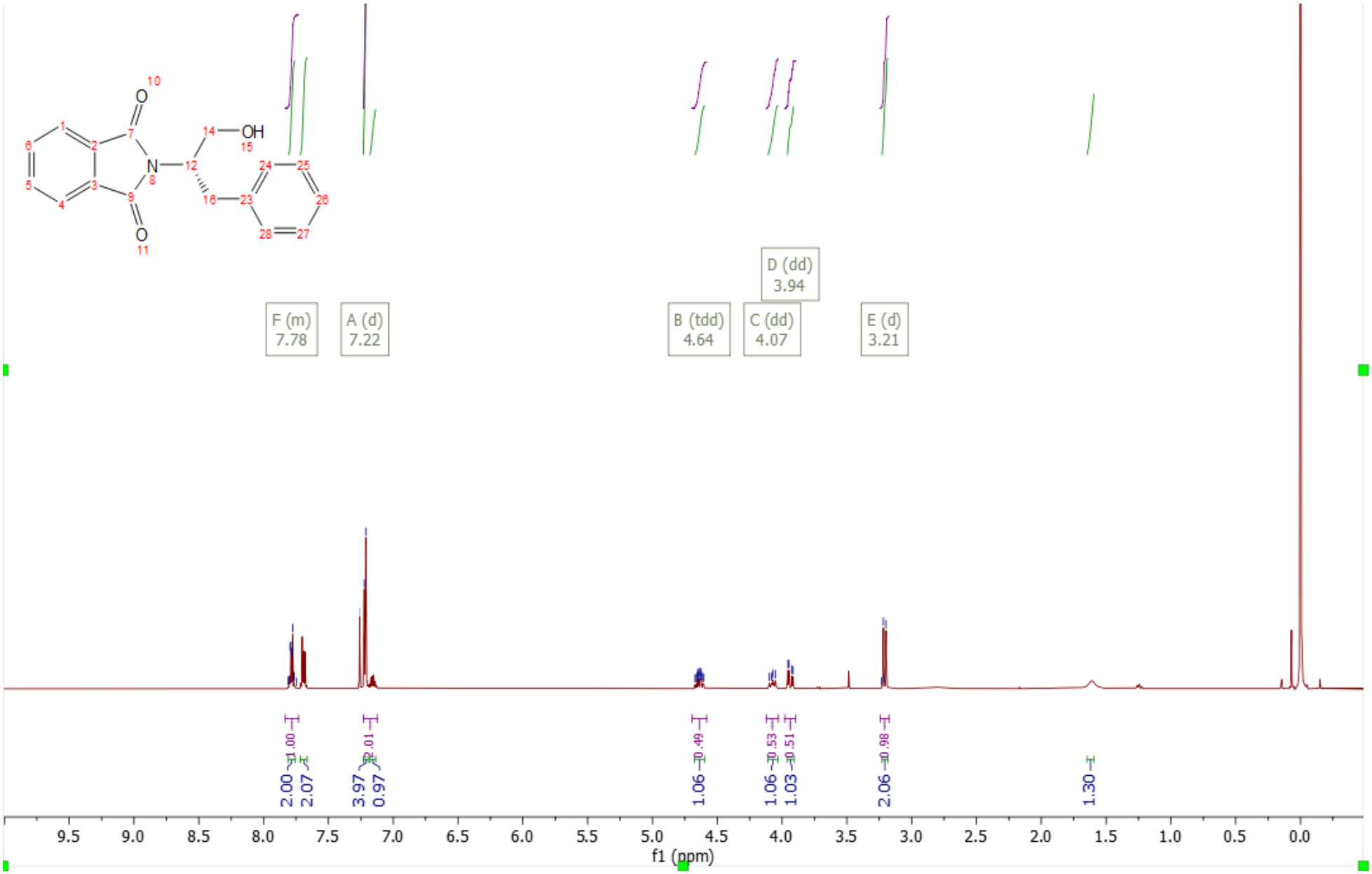

Compound 22 - 1-(tert-Butoxycarbonyl) indoline

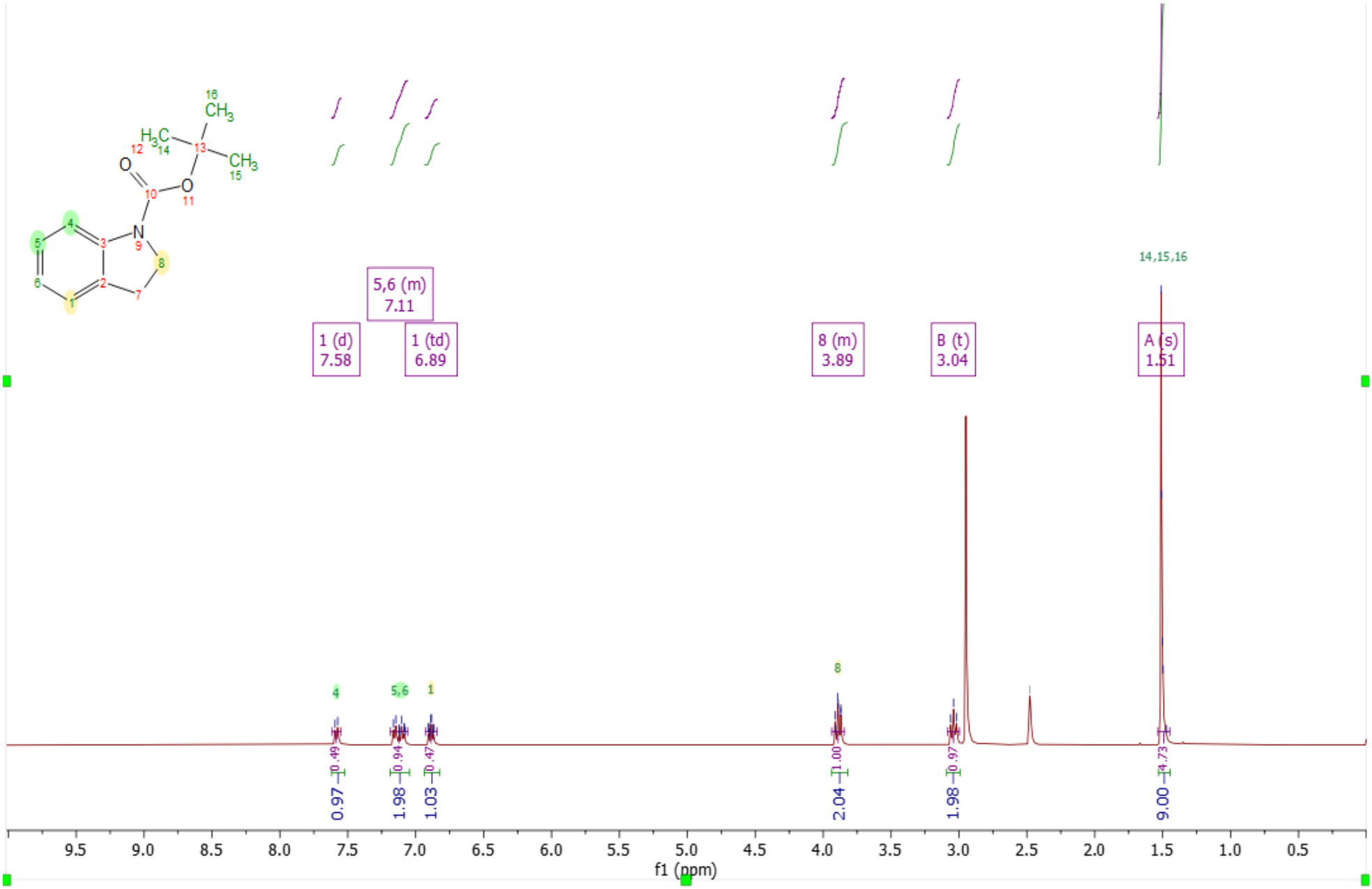

Compound 23 - (1,1-Dimethylethyl) 7-methyl-2,3-dihydro-1H-indole-1,7-dicarboxylate

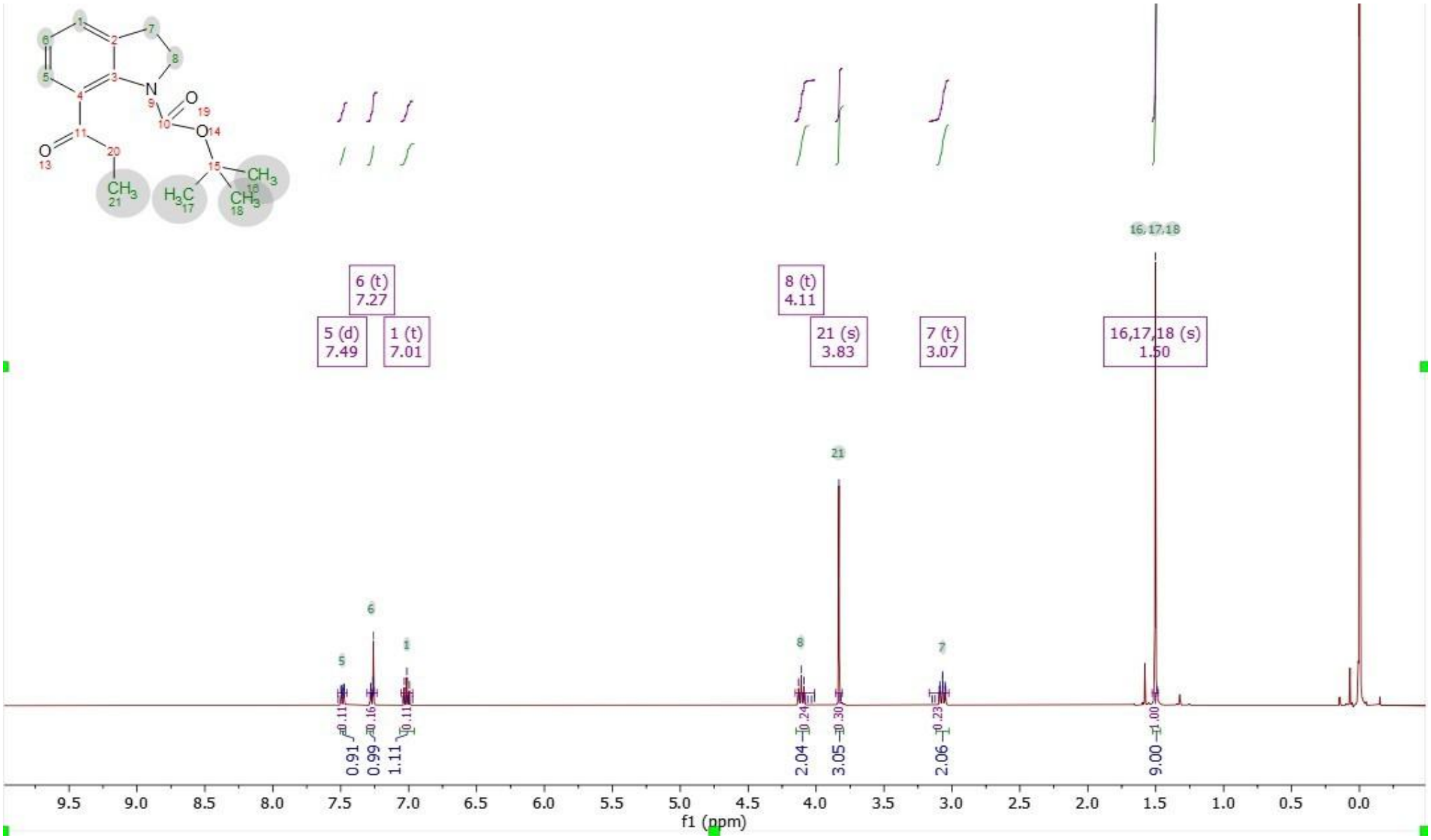

Compound 24 - 1-(1,1-Dimethylethyl)7-methyl-5-bromo-2,3-dihydro-1H-indole-1,7-dicarboxylate

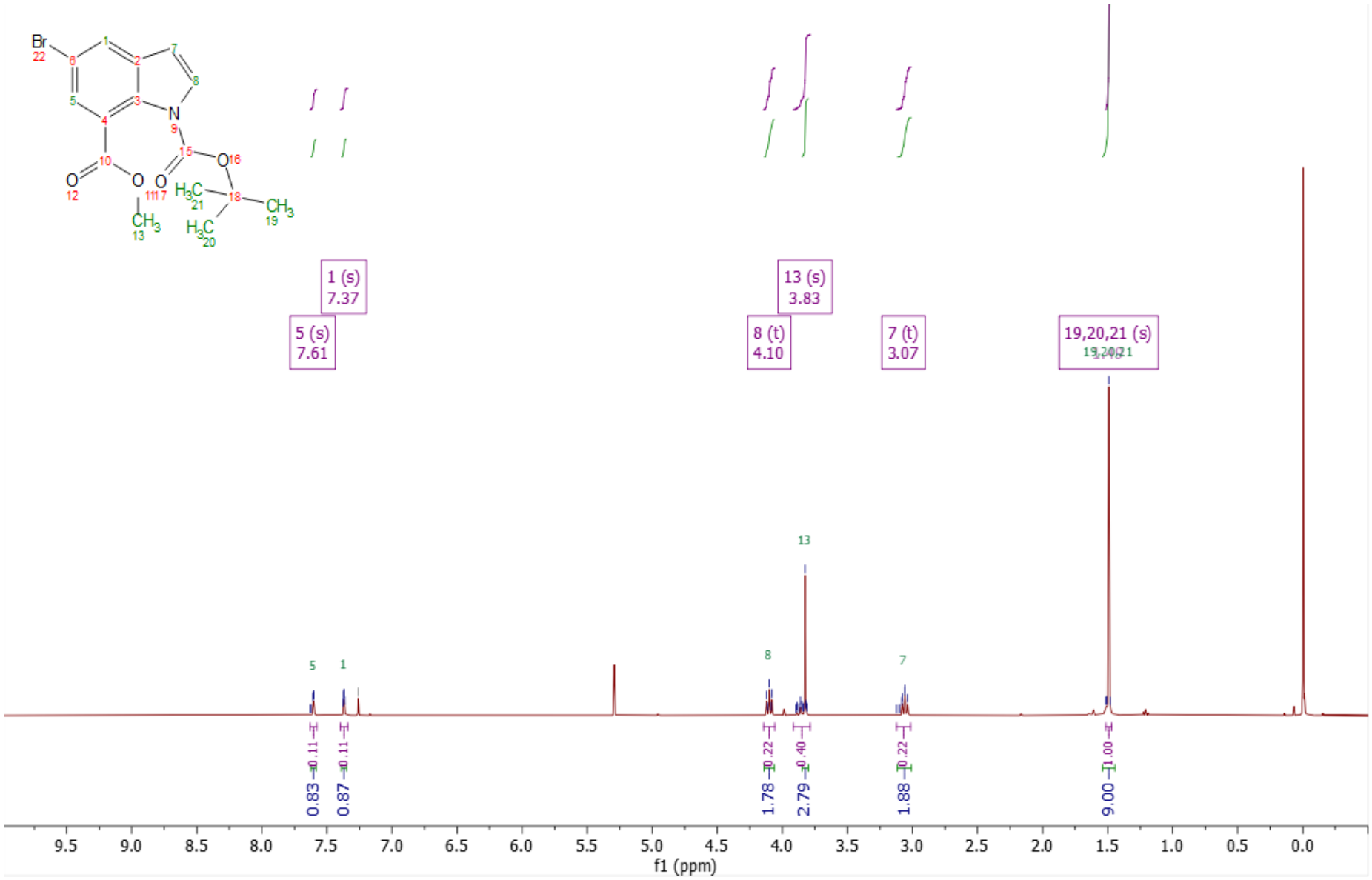

Compound 25 - 1-(1,1-Dimethylethyl)7-methyl-5-bromo-2,3-dihydro-1H-indole-1,7-dicarboxylate

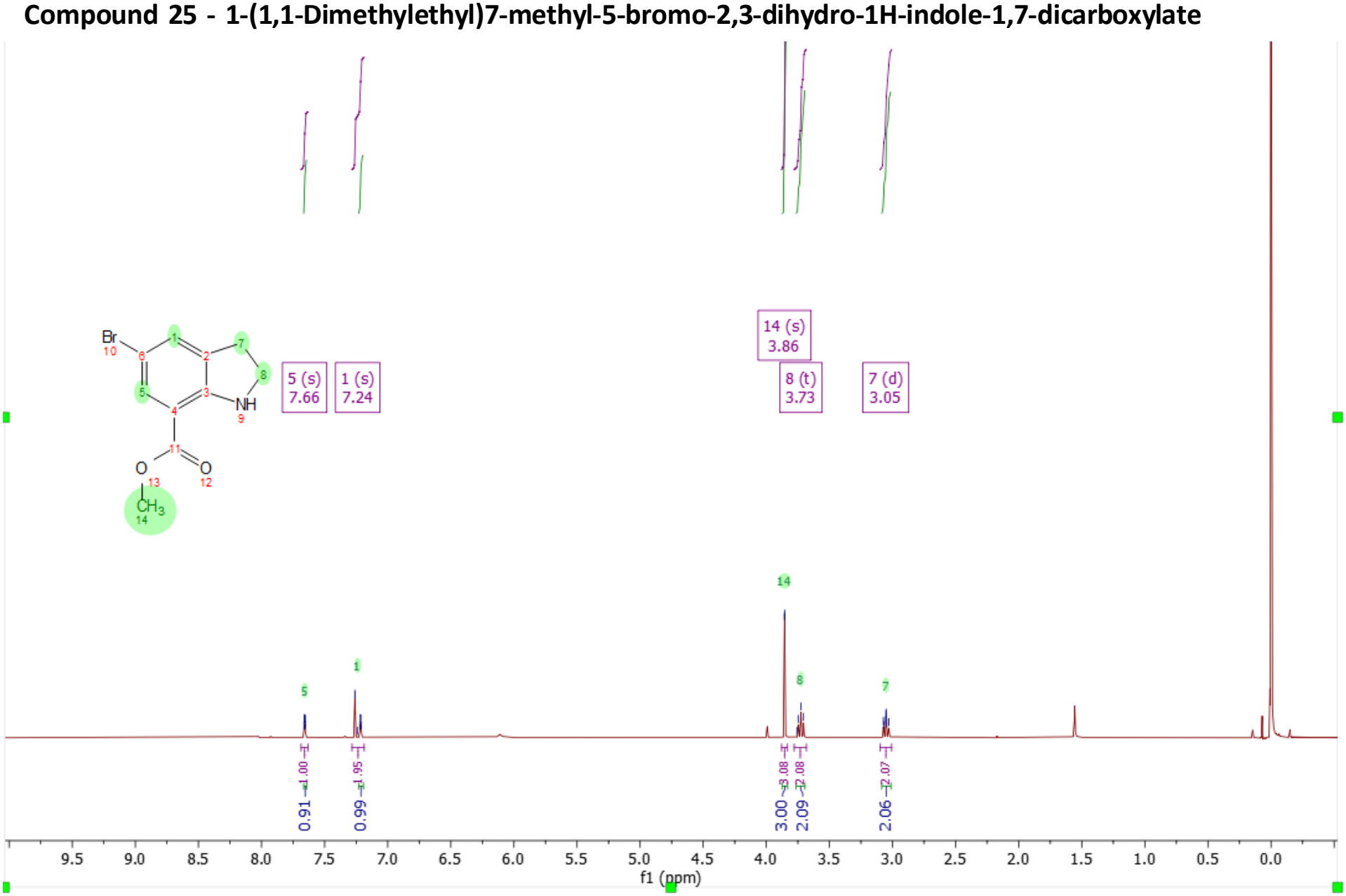

Compound 26 - Methyl-5-bromo-1H-indole-7-carboxylate

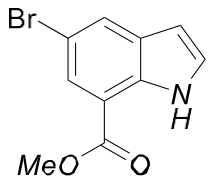

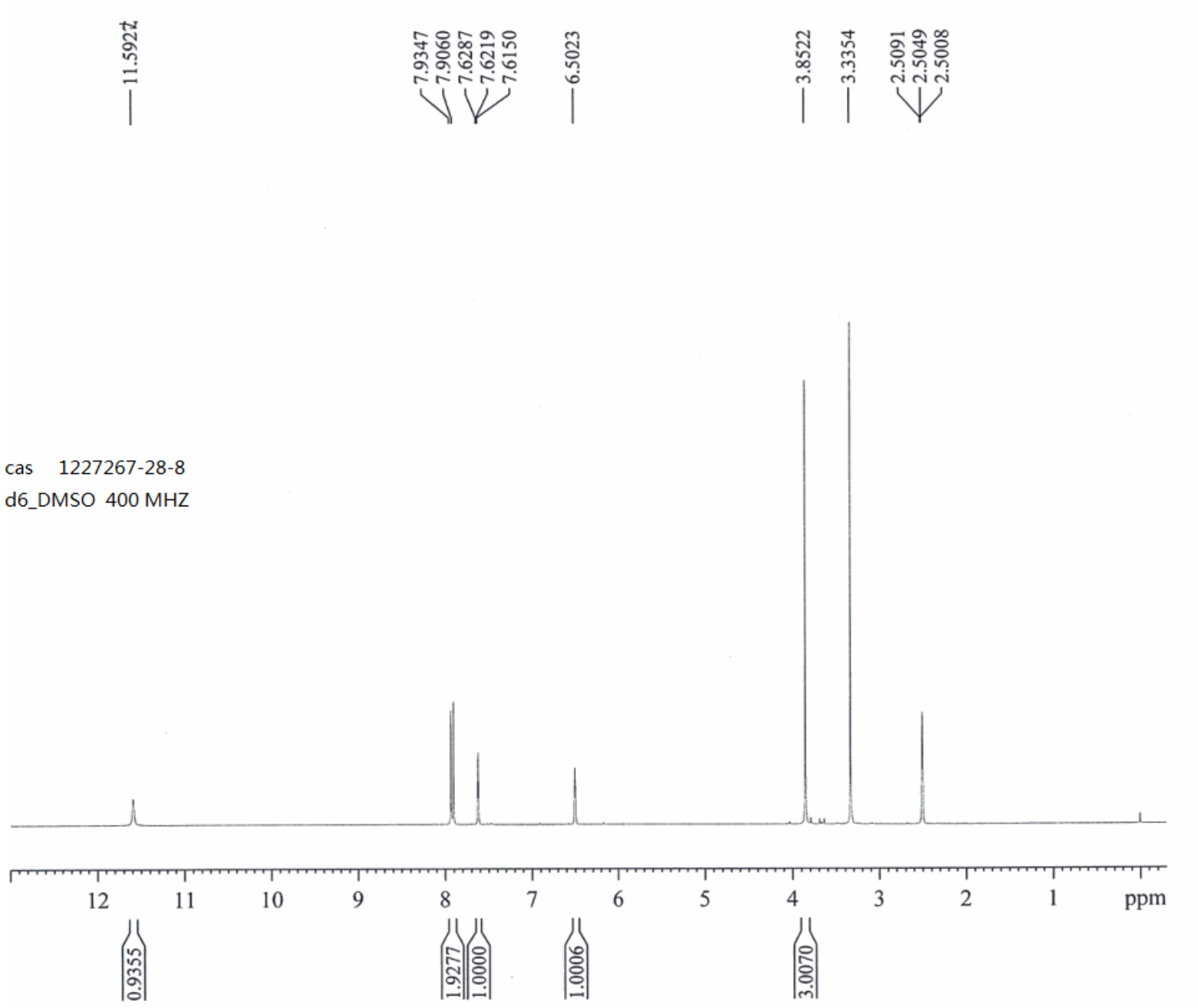

Figure 11 – H1 NMR Spectrum for methyl-5-bromo-1H-indole-7-carboxylate

Compound 27 - 5-Bromo-1H-indole-7-carboxylic acid

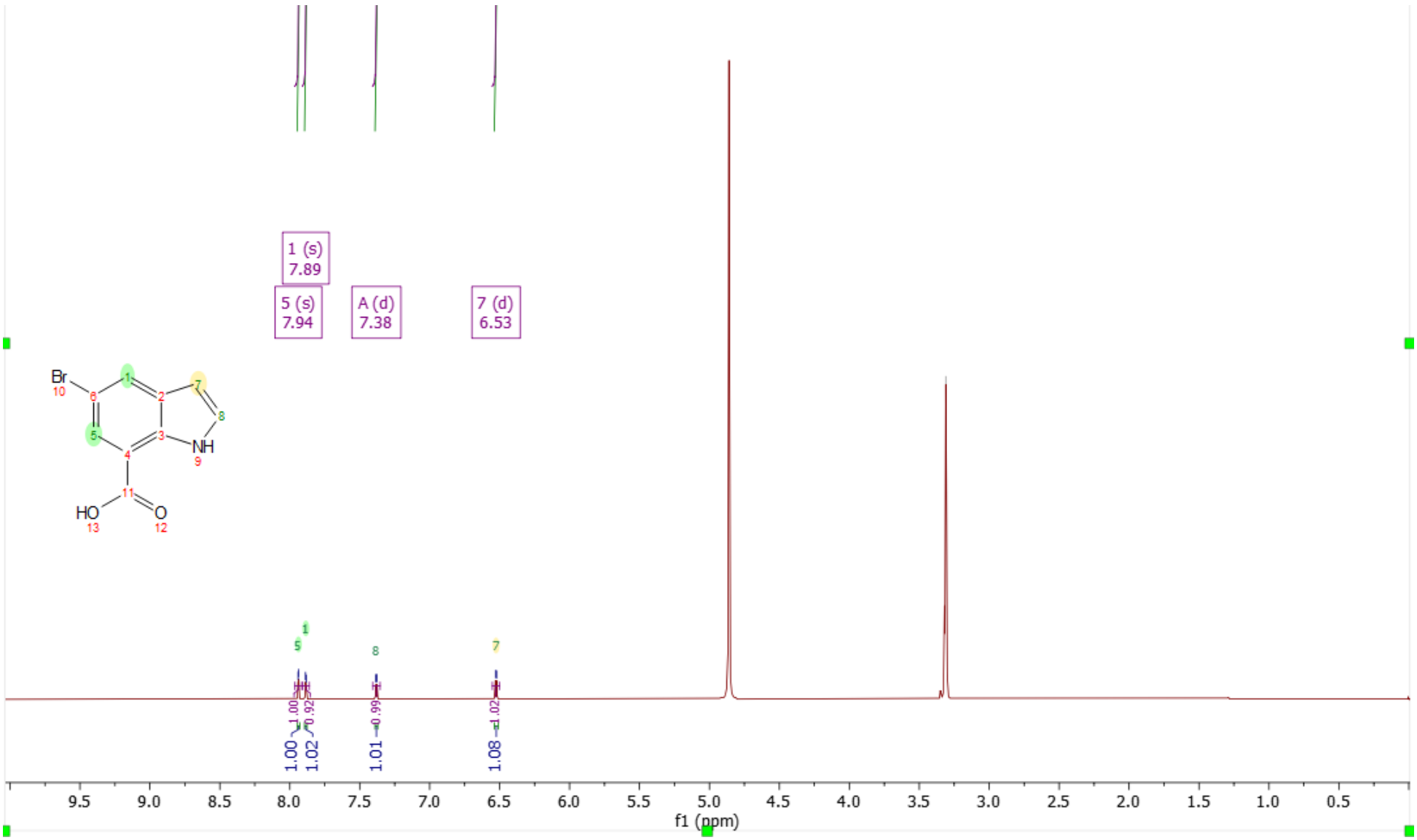

Compound 28 - 5-Bromo-1H-indole-7-carboxamide

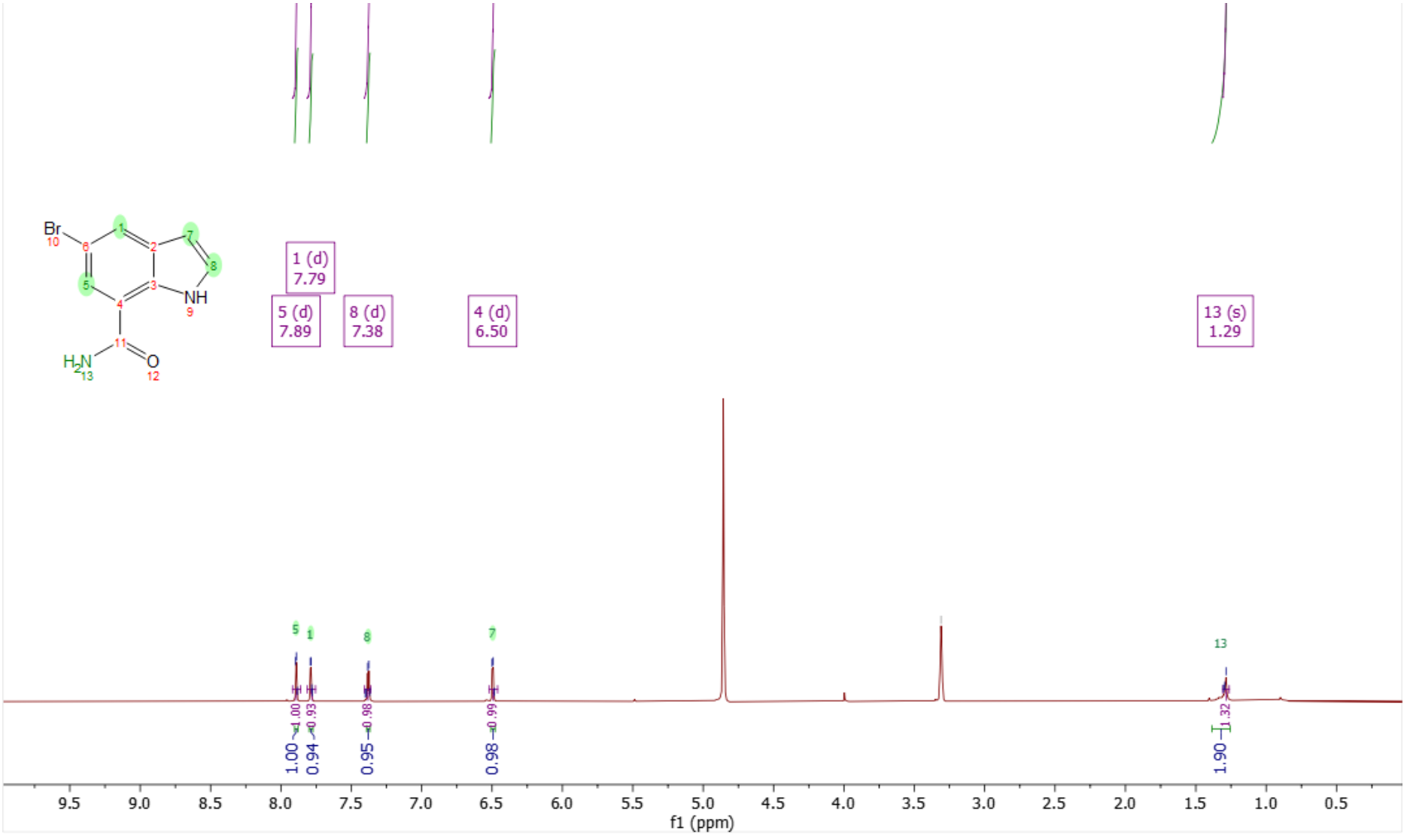

Compound 29 - 5-Pyrazole-1H-indole-7-carboxamid

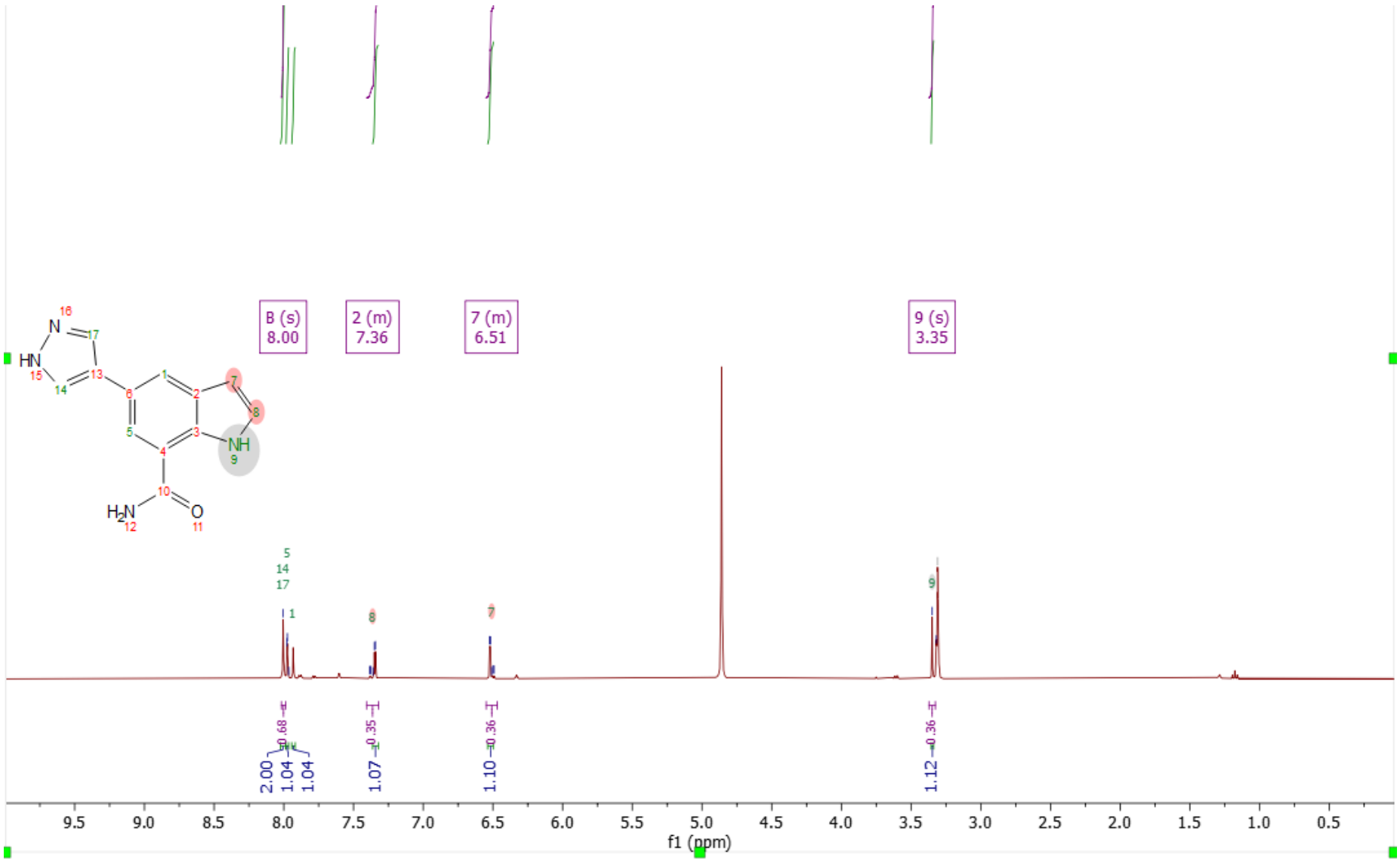

Compound 1 - LCMS- (S)-2-(1-hydroxy-3-phenylpropan-2-yl)isoindoline-1,3-dione

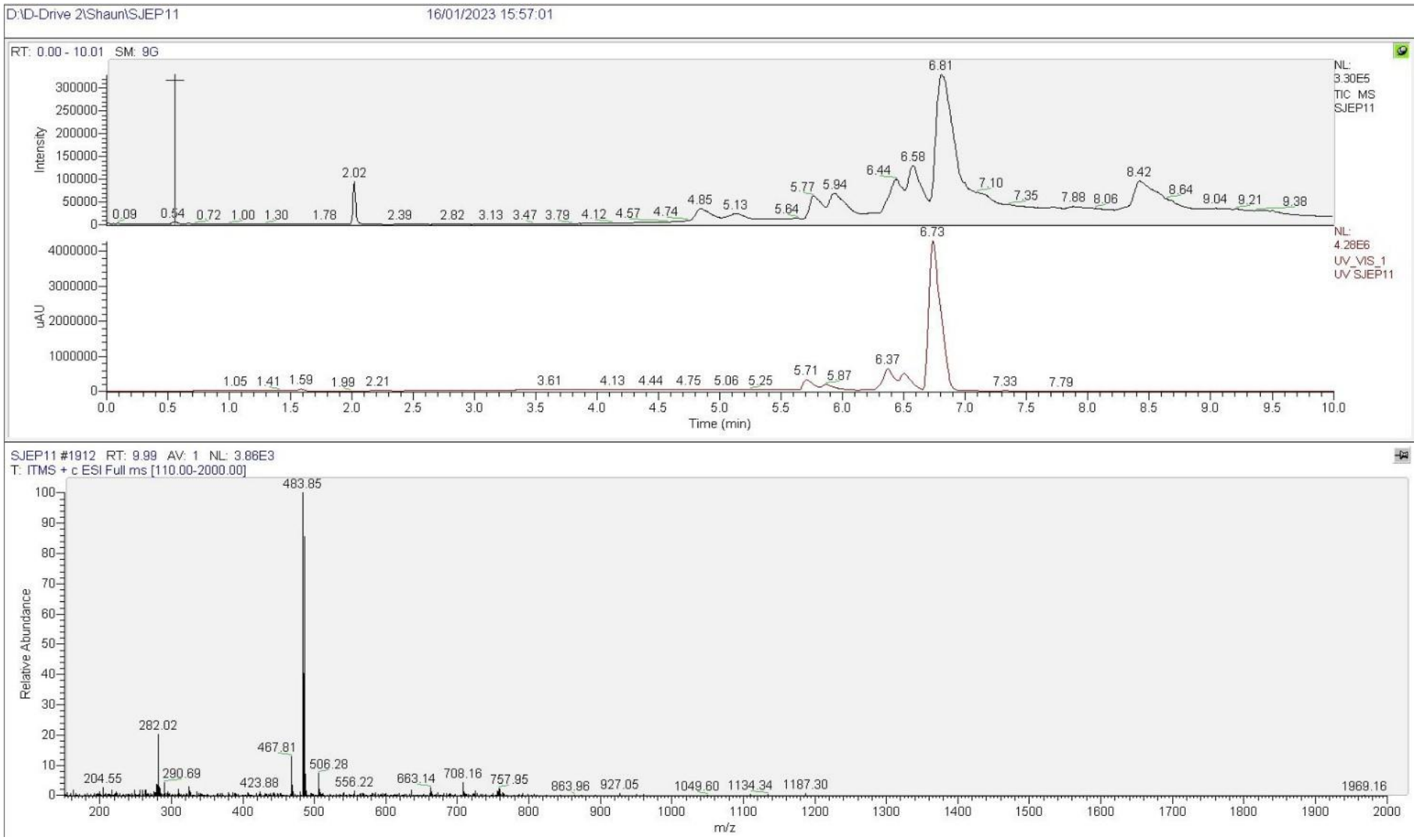

References

1 World Health Organization, Neglected tropical diseases -- GLOBAL, https://www.who.int/health-topics/neglected-tropical-diseases#tab=tab_1, (accessed 29 April 2025).

2 S. E. Ward and A. M. Davis, .

3 J. N. Burrows, C. B. Cooper, C. Mowbray and P. Sjö, in *The Handbook of Medicinal Chemistry: Principles and Practice*, eds. S. E. Ward and A. Davis, The Royal Society of Chemistry, 2023, p. 0.

4 W. Health Organization, *World malaria report 2022*, .

5 K. Habtamu, B. Petros and G. Yan, *Trop Dis Travel Med Vaccines*, 2022, **8**, 27.

6 A. Chiappino-Pepe, V. Pandey and O. Billker, *Curr Opin Microbiol*, 2021, **63**, 259–266.

7 A. Molina-Cruz, G. E. Canepa, N. Kamath, N. V. Pavlovic, J. Mu, U. N. Ramphul, J. L. Ramirez and Carolina Barillas-Mury, *Proc Natl Acad Sci U S A*, 2015, **112**, 15178–15183.

8 E. A. Ashley, A. Pyae Phyo and C. J. Woodrow, *The Lancet*, 2018, **391**, 1608–1621.

9 J. A. Simpson, R. Price, F. Ter Kuile, P. Teja-Isavatharm, F. Nosten, T. Chongsuphajaisiddhi, S. Looareesuwan, L. Aarons and N. J. White, *Clin Pharmacol Ther*, 1999, **66**, 472–484.

10 K. Haldar, S. Bhattacharjee and I. Safeukui, *Nat Rev Microbiol*, 2018, **16**, 156–170.

11 G. Li, H. Li, P. Wang, X. Zhang, W. Kuang, L. Huang, Y. Zhang, W. Xiao, Q. Du, H. Tang and J. Wang, *Cell Communication and Signaling* , 2025, **23**, 1–14.

12 C. M. Moore, J. Wang, Q. Lin, P. Ferreira, M. A. Avery, K. Elokely, H. M. Staines and S. Krishna, *Antimicrob Agents Chemother*, 2022, **66**, e02079-21.

13 W. Health Organization, *Artemisinin resistance and artemisinin-based combination therapy efficacy (December 2018)*, .

14 J. Wang, C.-J. Zhang, W. Ni Chia, C. C. Loh, Z. Li, Y. Mun Lee, Y. He, L.-X. Yuan, T. Kwang Lim, M. Liu, C. Xia Liew, Y. Quan Lee, J. Zhang, N. Lu, C. Teck Lim, Z.-C. Hua, B. Liu, H.-M. Shen, K. S. Tan and Q. Lin, Nat Commun, 2015, 6, S011

15 M. Rudrapal and D. Chetia, *Drug Des Devel Ther*, 2016, **10**, 3575–3590.

16 D. N. Dhanasekaran and E. Premkumar Reddy, *Genes Cancer*, 2017, **8**, 682–694.

17 S. K. Hanks and T. Hunter, *The FASEB Journal*, 1995, **9**, 576–596.

18 I. Yeh, T. Hanekamp, S. Tsoka, P. D. Karp and R. B. Altman, *Genome Res*, 2004, **14**, 917.

19 F. Joubert, C. M. Harrison, R. J. Koegelenberg, C. J. Odendaal and T. A. P. De Beer, *Malar J*, 2009, **8**, 1–8.

20 D. L. Doolan, C. Dobaño and J. K. Baird, *Clin Microbiol Rev*, 2009, **22**, 13–36.

21 L. von Seidlein and J. L. Deen, *The Lancet*, **373**, 522–523.

22 S. Kumar, O. R. Gargaro and S. H. I. Kappe, *mBio*, 2022, **13**, e02227-22.

23 M. M. Alam, A. Sanchez-Azqueta, O. Janha, E. L. Flannery, A. Mahindra, K. Mapesa, A. B. Char, D. Sriranganadane, N. M. B. Brancucci, Y. Antonova-Koch, K. Crouch, N. V. Simwela, S. B. Millar, J. Akinwale, D. Mitcheson, L. Solyakov, K. Dudek, C. Jones, C. Zapatero, C. Doerig, D. C. Nwakanma, M. J. Vázquez, G. Colmenarejo, M. J. Lafuente-Monasterio, M. L. Leon, P. H. C. Godoi, J. M. Elkins, A. P. Waters, A. G. Jamieson, E. F. Álvaro, L. C. Ranford-Cartwright, M. Marti, E. A. Winzeler, F. J. Gamo and A. B. Tobin, *Science*, 2019, **365**, eaau1682–eaau1682.

24 A. Mahindra, O. Janha, K. Mapesa, A. Sanchez-Azqueta, M. M. Alam, A. Amambua-Ngwa, D. C. Nwakanma, A. B. Tobin and A. G. Jamieson, *J Med Chem*, 2020, **63**, 9300–9315.

25 C. Abad-Zapatero and J. T. Metz, *Drug Discov Today*, 2005, **10**, 464–469.

26 C. A. Lipinski, F. Lombardo, B. W. Dominy and P. J. Feeney, *Adv Drug Deliv Rev*, 2001, **46**, 3–26.

27 M. L. Verdonk, I. Giangreco, R. J. Hall, O. Korb, P. N. Mortenson and C. W. Murray, *J Med Chem*, 2011, **54**, 5422–5431.

28 A. L. Hopkins, C. R. Groom and A. Alex, *Drug Discov Today*, 2004, **9**, 430–431.

29 N. Neerathilingam, S. Prabhu and R. Anandhan, *Org Biomol Chem*, 2023, **21**, 7707–7711.

30 Mitsunobu Reaction, https://www.organic-chemistry.org/namedreactions/mitsunobu-reaction.shtm, (accessed 9 June 2025).

31 Suzuki Coupling, https://www.organic-chemistry.org/namedreactions/suzuki-coupling.shtm, (accessed 9 June 2025).

32 J. K. Kerns, J. Busch-Petersen, W. Fu, J. C. Boehm, H. Nie, M. Muratore, A. Bullion, G. Lin, H. Li, R. Davis, X. Lin, A. S. Lakdawala, R. Cousins, R. Field, J. Payne, D. D. Miller, P. Bamborough, J. A. Christopher, I. Baldwin, R. R. Osborn, J. Yonchuk, E. Webb and W. L. Rumsey, *ACS Med Chem Lett*, 2018, **9**, 1164–1169.

33 Boc-Protected Amino Groups, https://www.organic-chemistry.org/protectivegroups/amino/boc-amino.htm, (accessed 9 June 2025).

34 J. M. Muchowski and M. C. Venuti, *Journal of Organic Chemistry*, 1980, **45**, 4798–4801.

35 Boc Protecting Group: N-Boc Protection & Deprotection Mechanism –, https://total-synthesis.com/boc-protecting-group/, (accessed 11 June 2025).

36 S. M. Bauer and R. W. Armstrong, *J Am Chem Soc*, 1999, **121**, 6355–6366.

37 N. Miyaura, K. Yamada and A. Suzuki, *Tetrahedron Lett*, 1979, **20**, 3437–3440.

38 A. Mahindra, *Experimental for synthesis of JZ208105-178D1*, .